Tracking thorium-234 to study particle dynamics in a coastal hypersaline lagoon: implications for environmental degradation in Mar Menor (SE Spain)

Treball Final de Grau

Grau en Ciències Ambientals, Facultat de Ciències

Marina Miralles Vidal, Paula Mostazo Alsina

Tutores: Aaron Alorda Kleinglass, Montserrat Roca Martí

26 juny 2024

UAB Universitat Autònoma de Barcelona

ICTA Institute of Environmental Science and Technology - UAB

AGRAÏMENTS

En primer lloc agrair a les nostres tutores, Muntsa i Aaron, per convidar-nos a contribuir en una petita part en el projecte WINDERS, deixar-nos formar part de la campanya de recollida de mostres i donar-nos llibertat per aprendre i equivocar-nos al llarg del procés; des de la presa de mostres i el processament d'aquestes al laboratori fins a la redacció i elaboració d'aquest treball final de grau. En especial gràcies per tots els consells i per la paciència.

Agrair també al Departament de Física de Radiacions de la UAB per deixar-nos les instal·lacions, material i instruments que han fet possible que aquest projecte surti endavant.

Volem fer una menció especial a les amigues que ens emportem d'aquesta etapa, sense el suport de totes no hauríem arribat fins al final, Ainhoa, Gemma, Laura i Paula mil gràcies per tots i cadascun des moments viscuts al llarg d'aquests cinc anys.

Finalment agrair a tothom qui ha contribuït d'alguna manera en aquest projecte, idees, coneixement d'Excel, suport i motivació, totes iguals d'importants. Gràcies per fer que el desenvolupament d'aquest estudi en els darrers mesos hagi estat un camí més fàcil i enriquidor.

CONTENTS

ABSTRACT

Coastal lagoons are complex socio-ecological systems that sustain biodiversity as well as several economical activities. Their over-exploitation has caused a rapid degradation in the last decades. Understanding the dynamics and complexity of coastal lagoons is a must to be able to protect these habitats. Radioactive isotopes have been widely used as tracers to track, measure and quantify a wide range of environmental processes in aquatic systems. For instance, the pair of radionuclides thorium-234/uranium-238 (^{234}Th/^{238}U), due to its physicochemical characteristics, is very useful for tracking the movement of particles in the open ocean. However, it has been recently suggested as potential tool to use in coastal areas. Although the use of ^{234}Th/^{238}U pair in these areas may have limitations, it could be a potential tool for studying particle fluxes and particle dynamics in shallower waters.

The Mar Menor lagoon (SE Spain), is one of the biggest hypersaline coastal lagoons in the Mediterranean Sea and harbors the habitat of endangered species. Mar Menor has suffered in the past from eutrophication and anoxic conditions as it has historically been a heavily human-pressured environment. Eutrophication events are triggered by torrential rains as well as submarine groundwater discharge as they supply enormous amounts of nutrients and particles which are net contributors to devastating algal blooms in the lagoon. However, resuspension has lately been proposed to be another contributor that causes the algae blooms, so this study aims to assess if ^{234}Th/^{238}U pair could be a potential tracer for resuspension in Mar Menor. To route this innovative line of study on ^{234}Th/^{238}U, a field campaign was conducted in Mar Menor lagoon from January 25th to February 1st, 2024. Background physicochemical data was recorded daily during the campaign by local authorities. This data was used in combination with three different types of samples (i.e., water samples, sediment traps and sediment cores) which were collected in four sampling stations.

The results varied among the types of samples. On the first hand, water samples results reflected a large quantity of particles along the water column and stations. This hypothesis is supported by the high turbidity measured throughout the water column 2 days before sampling, and thus enhancing the presence of particles along the water column. On the other hand, sediment traps and cores samples showed a different trend depending on the stations. Regarding sediment traps samples, the westernmost station recorded higher values of ^{234}Th flux and sedimentation rate, probably because of a turbidity event during sample collection that only affected that station. Finally, sediment core samples showed no potential evidence to recent sedimentation in this same station as it is located in an area characterized by particle dragging and not sedimentation processes.

This study has made it possible to collect information about particle dynamics in Mar Menor by the early 2024. A new path of research could be open for ^{234}Th/^{238}U as a tool to potentially track particle fluxes in shallow water systems. Results seen are consistent enough to prove ^{234}Th as an effective particle tracer in Mar Menor since our findings suggest evidence for both vertical and horizontal particle fluxes. Nevertheless, no clear sign of resuspension was found. Finally, considering some limitations were found, recommendations for future research are suggested. Since there are not many studies in this field, this pilot study aims to pave the way for newer applications.

1 INTRODUCTION

Oceans cover nearly 70% of planet Earth surface, that's why many authors throughout history refer to it as The Blue Planet. However, it is the most unexplored place in the whole planet having only properly studied around 5% of this enormous water body. In the last few decades, ocean dynamics and marine ecosystems have been the main research focus for thousands of experts enthralled by them. Not only large oceans but also smaller water masses like coastal lagoons have been in the spotlight for researchers trying to understand their complexity and essential role in biodiversity and planet's health. Coastal lagoons are complex social-ecological systems with ecosystem services that provide livelihoods, wellbeing, and welfare to humans (Newton et al., 2018), therefore its conservation and natural preservation it is not only important for ecosystem protection but also for human interests. Because coastal lagoons are an important source for the development of human activities, their over-exploitation has caused their rapid degradation in the last decades transforming rich ecosystems into polluted ones. The need to understand the dynamics of these sites is essential to achieve effective planning for their protection and thus ensure the recovery of these key ecosystems.

To reach these goals, many techniques have been developed in order to study different processes in aquatic systems. One of which are radionuclides, radioactive isotopes present in our planet in extremely low concentrations but powerful enough to be tracked (Rodellas et al., 2023). The wide range of naturally occurring radionuclides have become a multidisciplinary instrument to study many ocean processes which are usually difficult to measure and quantify. The main processes that have been studied with radionuclides include: **ocean circulation**, i.e., the movement of water masses and fluxes of particulate or dissolved material; **atmosphere and land interaction with oceans**, i.e., riverine and groundwater discharge, weathering or diffusion from deposited sediments, air-sea gas exchange processes or atmospheric deposition; and **sedimentation processes,** i.e., sedimentation rates and dating (Rodellas et al., 2023).

One of the most used tools is the relation between parent/daughter radionuclides pairs from the same decay chain. When one radionuclide (parent isotope) decays into another radionuclide (daughter isotope), it also decays into another isotope (stable or unstable) and forms a decay chain (Rodellas et al., 2023). In this study, the uranium-238 (^{238}U) and thorium-234 (^{234}Th) pair are used. ^{238}U, the parent isotope, becomes ^{234}Th (daughter isotope) via alpha decay. The ^{234}Th/^{238}U pair has been widely used for many years as a particle tracer since Bhat et al. (1969) started studying ^{234}Th scavenging[1] in seawater. ^{234}Th is a short-lived (half-life, $T_{1/2}$ = 24.1 days) naturally occurring isotope and ^{238}U is a long-lived radionuclide ($T_{1/2}$= 4.5 10^9 years). Therefore, ^{238}U decays at a much slower rate than its daughter, which means that if ^{234}Th was only added or removed from the system by radioactive decay, both parent and daughter would reach secular equilibrium (i.e., the activities of both radionuclides would be the same). Still, since in this specific case the daughter isotope ^{234}Th has a higher particle reactivity than its parent ^{238}U, particle scavenging leads to the removal of ^{234}Th from seawater (Cochran et al., 1995), producing a disequilibrium in the upper water column (Figure 1.A) where ^{234}Th activities are lower than ^{238}U activities (Rodellas et al., 2023). Furthermore, apart from

[1] Scavenging of particle-reactive elements is the process of the removal of a dissolved element in seawater by adsorption onto sinking particulate matter. Scavenging is an important pathway for the transfer of nutrients and trace elements in the ocean. Radioactive isotopes are useful tools to provide constraints on the scavenging and organic particle removal processes (Maderich et al., 2022).

these processes causing ^{234}Th deficit (i.e., ^{234}Th < ^{238}U activities) in the upper water column, some studies reveal ^{234}Th deficit near to bottom sediments are probably caused by particle resuspension (Figure 1.A and 1.B, Aller & Cochran, 1976; Muir et al., 2005; Santschi et al., 1979).

The difference in half-lives and particle affinity between ^{238}U and ^{234}Th (Moore & Hunter, 1985), makes this pair an ideal tool for tracing scavenging processes occurring in timescales of days to months (Bhat et al., 1969; Buesseler et al., 2006; Cochran et al., 1995; Cochran & Masqué, 2003; Moore & Hunter, 1985; Muir et al., 2005; Owens et al., 2015).

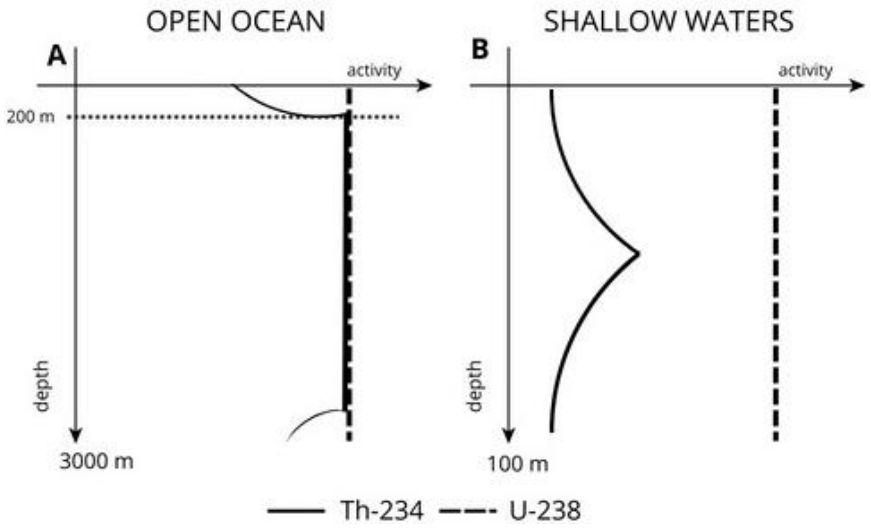

Figure 1. Schematic diagram of the hypothetical activity of ^{234}Th and ^{238}U throughout depth in A. open ocean and B. shallow waters. Adapted from Black et al. (2024).

The main natural aquatic processes in which this method is applied are: **vertical transport** (i.e., vertical movement of particles in the water column), **horizontal transport** (i.e., horizontal movement of particles in systems with rapid advective flows), **particle cycling** (i.e., particle production, aggregation or disaggregation, sinking, decomposition or remineralization, and resuspension; Amaral et al., 2022) and **sediment dynamics** (i.e., sedimentation, bioturbation, physical resuspension and mixing) (Waples et al., 2006). Moreover, the combination of these processes offers quantitative information about the biological carbon pump (BCP) and the marine carbon cycle (Rodellas et al., 2023). According to De La Rocha & Passow (2014), the BCP is the set of processes by which inorganic carbon is fixed into organic matter via photosynthesis and then sequestered away from the atmosphere into the deep ocean performing a great role in buffering the global climate system (Le Moigne et al., 2013). One of the methods to quantify its importance is estimating vertical particulate organic carbon (POC) fluxes from the surface to the deep ocean (Boyd et al., 2019; Buesseler et al., 2006, 2020; Cochran et al., 1995; Le Moigne et al., 2013; Owens et al., 2015).

Beyond the application of the ^{234}Th/^{238}U method in the open ocean, a new path for research is now open for shallow waters. Recently, Black et al. (2023) has used the ^{234}Th/^{238}U pair to estimate vertical carbon fluxes from the water column to the surface sediments in a semi-restricted coastal basin (Beford basin, Canada) and has put forth a future research path for using this method to study sediment resuspension and its potential impact on coastal carbon budgets. The possibility of implementing the ^{234}Th/^{238}U technique in shallow water columns (tens of meters deep) could be used for tracing particulate matter related to anthropic activities in coasts, and other salty shallow water masses.

Coastal areas, which include both continental and aquatic ecosystems, cover only around 8% of the global surface area but account for as much as 25% of global primary production (Turner et al., 1996) and are home to over 60% of the world's population (Lakshmi & Rajagopalan, 2000). Historic human intervention and over-exploitation of resources such as fisheries as well as changes in land use and urbanization, have caused coastal areas degradation, via polluting directly or modifying climate dynamics, and overall contributing to climate change and the rising of sea levels (Turner et al., 1996).

To route this innovative field, the Spanish Mar Menor coastal lagoon has been selected in this study to carry on the application of the $^{234}Th/^{238}U$ technique in shallow water columns. The Mar Menor lagoon, located in Cartagena, Murcia (SE Spain), is one of the biggest hypersaline coastal lagoons in the Mediterranean Sea (Conesa & Jiménez-Cárceles, 2007). The Mar Menor lagoon is part of the ZEPIM[2] (*Zonas Especialmente Protegidas y de Importancia para el Mediterraneo;* MITECO, 1999) because it harbors specific ecosystems of the Mediterranean area or habitats of endangered species. ZEPIM areas, according to the Spanish Ministry of Ecological Transition and Demographic Challenge are important for the conservation of the biological diversity in the Mediterranean, which has special scientific, aesthetic, cultural or educational interests (MITECO, 1999). However, its strategic location, climate and natural resources have stimulated the development of anthropogenic activities especially: mining, agriculture, and tourism (Conesa & Jiménez-Cárceles, 2007), and thus creating a high nutrient environment which has put at stake Mar Menor's conservation.

Mining exploitation in Sierra de Cartagena started with the Roman Empire but had its main activity during the 19th and 20th centuries (Oyarzun et al., 2013). The prolonged and continuous exportation and the torrential rains dragging the mineral waste have caused the accumulation of heavy metals in the lagoon. Agriculture-related chemicals coming from Campo de Cartagena through the streams, have also been found in the Mar Menor. Finally, the most recently developed activity in this area has been tourism which has resulted in an overexpansion of the housing development in La Manga, leaving a highly touristic (and degraded) ecosystem.

Each of the three economic activities developed in the outskirts of the lagoon have been for many decades or even centuries the origin of heavy metals; coming from the mining exploitation, and nutrients; related to agriculture chemicals and wastewater from the incoming tourist population, accumulating in the lagoon. Moreover, illegal water management containing waste from agricultural and touristic activities (Tudela & Delgado, 2019), also supplies large amounts of nutrients.

Consequently, the development of economic activities in the Mar Menor, the waste they produce and the transport mechanisms from the source to the lagoon cause heavy phytoplankton proliferation (Fernández et al., 2013), also known as, episodes of eutrophication. Eutrophication creates algae blooms and thus, anoxic conditions (Fernández & Esteve Selma, 2007). Oxygen deficit causes several ecological impacts in the living organisms of the Mar Menor. This scenery throughout the decades has caused many eutrophication events in the lagoon. Examples of the heaviest events recorded were during 2015, 2019 and the most recent one in August 2021 where not only water in the lagoon turned green but it also caused mass fish deaths due to the anoxic conditions (Tudela & Delgado, 2019), an ecological disaster covered by both national and international press due to several local demonstrations.

All this waste generated from the different socio-economical activities reach the lagoon through streams, especially due to torrential rains episodes rapidly dragging this material and concentrating it

[2] In English referred as Special Protected Area of Mediterranean Interest (SPAMI)

into the lagoon, and subterranean groundwater discharge (SDG). But recently, **resuspension** has also been suggested as a possible triggering factor for the arrival in the water column of nutrients and heavy metals. Furthermore, Santos-Echeandía et al. (2023) carried out a study in Mar Menor determining wind as a key driver for resuspension events that could supply particulate material and nutrients to the lagoon.

The development of a technique to quantify and easily track the movement of particulate matter, as resuspension, and eventually POC, in coastal lagoons could potentially help understand the cycling of nutrients in such systems and possibly avoid or predict ecological disasters. Considering the singular aspects of Mar Menor and its ecological context, applying the $^{234}Th/^{238}U$ technique could provide new information about the lagoon and the method itself. This study will focus on evaluating the effectiveness of using ^{234}Th as particle tracer in Mar Menor, in particular of resuspension, which will potentially become a new path for future research.

2 OBJECTIVES

The aim of this study is to track particulate matter using the ^{234}Th technique in Mar Menor to develop a new application for this tool in shallow waters. ^{234}Th could potentially be effective in this area to study particle dynamics like resuspension, in order to prevent environmental degradation related to anthropic activities. To be able to achieve this goal, the specific objectives of this study are:

- Quantifying $^{234}Th/^{238}U$ disequilibrium in seawater and determining ^{234}Th activities in particulate samples (sediment traps and sediment cores) collected at different sites in Mar Menor to track particle movement in the lagoon.
- Contextualizing the water column data with the information from particulate samples taken at different sites in the lagoon, as well as high-frequency physicochemical measurements to explain the relation between meteorological phenomena, particle fluxes and water chemistry at the time of sample collection.
- Comparing the data obtained from different sites, types of samples, and possible environmental factors involved in the results obtained during the field work to assess whether ^{234}Th can be a suitable tracer for resuspension in Mar Menor.

3 METHODS

3.1. STUDY SITE

Mar Menor, located in Murcia (SE Spain), is one of the biggest hypersaline coastal lagoons in the Mediterranean Sea (Conesa & Jiménez-Cárceles, 2007). The lagoon is located in a quaternary plain belonging the geographical unit of Campo de Cartagena occasionally interrupted by volcanic outcrops as small islands (Conesa & Jiménez-Cárceles, 2007). It has a triangle shape with a surface area of 132 km^2, a perimeter of 59.51 km and a mean and maximum depth of 3.6 m and 6 m, respectively (Á. Pérez-Ruzafa et al., 2005) (Figure 2).

The lagoon is supplied by both riverbeds and by the Mediterranean Sea via three channels, as it is separated from the sea by a 20 km sand barrier called *La Manga*. *La Manga* is divided by a natural channel (*Encañizadas*) that isolates a natural protected area (*Salinas de San Pedro*) in the north from

the highly touristic area. Moreover, the urbanised area is disjoined by two artificial channels, *El Estacio* and *Marchamalo* (Figure 2). Several streams discharge in Mar Menor, which, although are usually inactive, when it rains carry considerable quantities of sediment from Cartagena-La Unión Mountain range (Velasco et al., 2006).

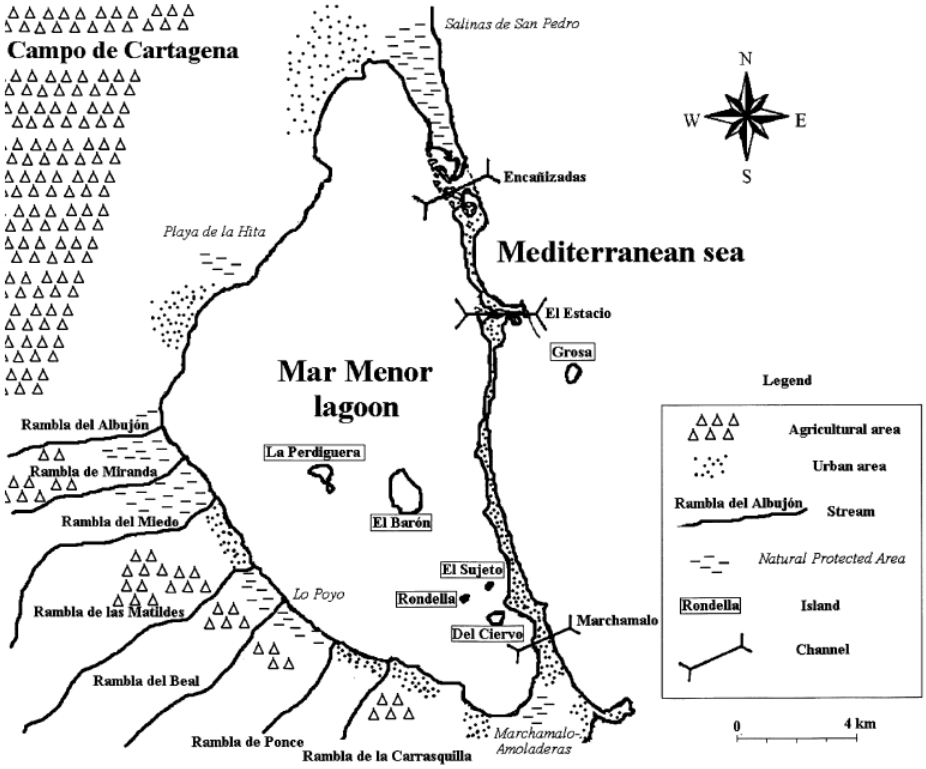

Figure 2. Schematic map of Mar Menor. Taken from Conesa & Jiménez-Cárceles (2007).

Murcia benefits from a Mediterranean climate, with long warm summers and mild winters (Köppen, 1936) and the precipitation is usually low but torrential during spring and autumn (Conesa & Jiménez-Cárceles, 2007). The water column of the coastal lagoon has a mean temperature of 20.5 ºC (period 2017-2024), ranging from 5 to 8 ºC during winter and from 30 to 31 ºC during summer (UPCT, 2024) (Figure 3.A). Moreover, it has an annual salinity of 42.33 PSU[3] (Figure 3.B) (Á. Pérez-Ruzafa et al., 2005). Oxygen has an inverse relation with water temperature and salinity (Figure 3.C). Mar Menor waters have usually constant parameters of oxygen throughout its shallow water column. Only bloom algae produce specific anoxic conditions (Fernández et al., 2013) like during the Mass Fish Death of August 2021.

The bed sediment grain size composition is predominantly muddy and sandy (Á. Pérez-Ruzafa et al., 2005). Moreover, salt marshes are present on the streams of the rivers, creating wetlands that have periodical phases of drying. These areas and their characteristics (i.e., salinity, temperature, wind patterns) are rich in unique flora and fauna[4] and thus have a very important ecological value (Conesa & Jiménez-Cárceles, 2007).

[3] PSU: Practical Salinity Unit

[4] For more information about flora and fauna in Mar Menor see Perez-Ruzafa (1989)

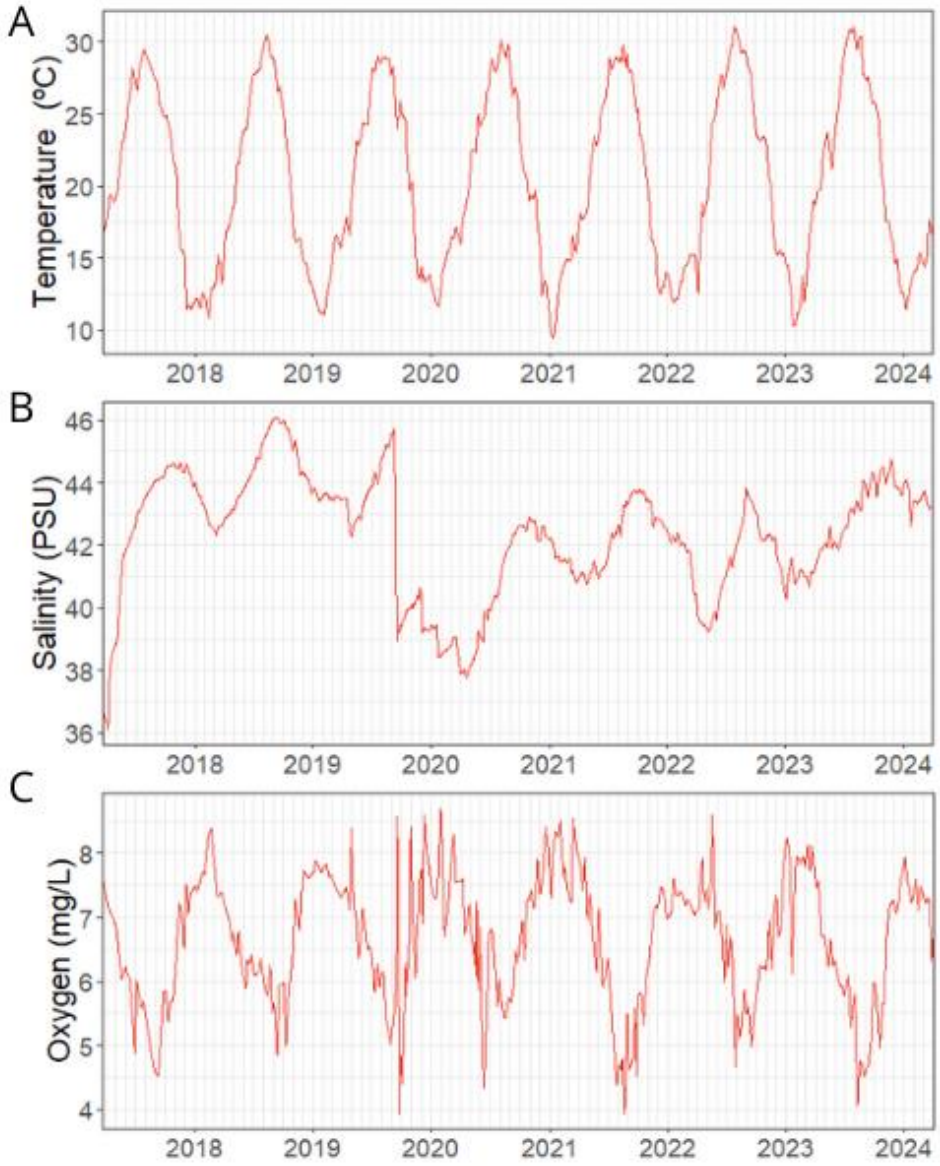

Figure 3. Daily variation of water temperature (A), salinity (B) and oxygen (C) since March 2017. Data obtained from: (UPCT, 2024), processed with Rstudio (RStudio Team, 2020).

As a result, the lagoon and the salt marshes have several protections: Ramsar International Site, ZEPIM, Site of Community Importance (SCI; Nature 2000 network: UE Habitats Directive), Specially Protected Area (SPA; CEE Birds Directive), and additional national and autonomic protective legislation. However, due to the anthropological pressure described above, these protections are not enough to preserve the ecological value Mar Menor.

Apart from its environmental interest, this area has historically been a strategic location for socio-economical activities development. The main ones: mining, agriculture and tourism have benefited from the lagoon resources and its strategical location.

Mining started with the Roman Empire and then developed especially during the second half of the 19th and 20th centuries in the Sierra de Cartagena (Oyarzun et al., 2013). Its main implications are related to tailings disposal dumped into the streams that drained the mining area (Conesa & Jiménez-Cárceles, 2007) and later arrival to the lagoon with the recurrent torrential rains occurring at the end

of the summer in the Mediterranean climate (Marín-Guirao et al., 2005; Á. Pérez-Ruzafa et al., 2005). Concentrations of metals like Pb, Zn and Cd found trapped in the sediments were higher than collected data from other points of the Spanish coast, creating a potential threat for living organisms in the lagoon and consequently affecting humans (Conesa & Jiménez-Cárceles, 2007).

The first evidence of human impact because of agricultural activities date back to around the 4th Century BC when the Roman Empire inhabited the Iberian Peninsula (Azuara et al., 2020). The first related activities consisted of dry farming, which, thanks to low water and fertilizer inputs, the resulting impacts were not severe (A. Pérez-Ruzafa et al., 2000). It was not until around 1980 that consequences from agriculture started to be noticeable, this fact is directly related to the interbasin transfer Tajo-Segura when a new era for intensive agriculture began in *Campo de Cartagena* (Caballero Pedraza et al., 2015). Among all impacts derived from irrigated intensive agriculture, it is important to consider landscape impact as well as consumption of resources and waste generation. Water is the most consumed resource in this kind of activities, where due to the climate in the region, groundwater exploitation has been a common practice, thus draining the coastal aquifer and inducing its salinization (Caballero Pedraza et al., 2015). Waste and fertilizers, especially nitrates and phosphorous compounds, flow into the lagoon through ravines and mainly through the *El Albujón* stream, which collects a large amount of the runoff waters from *Campo de Cartagena* (Caballero Pedraza et al., 2015). Lastly, it should be considered the proliferation of desalinization plants in the region, which may act as an additional source of pollution due to the dumped brine into the ravines (Conesa & Jiménez-Cárceles, 2007), which is rich in salts and nutrients (Martínez Fernández & Esteve Selma, 2003; Velasco et al., 2006).

Lastly, tourism has been the last activity to develop around the Mar Menor lagoon. The known real-state bubble (1998-2007) in the coastline of Murcia caused an expansive urbanism (Romero Díaz et al., 2017). The modification of the natural shoreline and the increase of residential population implied the loss of the characteristic dune systems as well as the disturbing of fauna, especially bird species (Conesa & Jiménez-Cárceles, 2007). Furthermore, in some areas, urban water treatments have important deficiencies that cause the discharge of highly rich nutrient wastewater into de coastal lagoon (Perez-Ruzafa & Aragón, 2002).

As said before, due to its geographical position, hydrogeological characteristics, and anthropogenic historical pressure, Mar Menor waters show episodes of abnormally high concentrations of nutrients, organic matter (OM) and other particulate matter. Both OM and nutrients, especially nitrogen and phosphorus, come from river runoff and subterranean discharge, especially after heavy rainfall episodes (Á. Pérez-Ruzafa et al., 2005; Perez-Ruzafa & Aragón, 2002). Those effluents concentrate in the almost isolated lagoon, creating a favorable environment for eutrophication. Moreover, heavy meteorological events need to be considered as a possible triggering factor of particle resuspension which can bring OM and nutrients previously deposited to sediments back to the water column therefore intensifying hypertrophic conditions.

3.2. CAMPAIGN

The sampling campaign was carried in 2024 from January 25th to February 1st. The sampling was done in four stations of Mar Menor, henceforth known as M1, M2, M3 and M4 (Figure 4, see Table 1 in Appendix section 8.1).

Figure 4. Location of the four stations marked as red dots.

On January 25th, water samples were collected at 1 m resolution from the surface to the bottom using a battery-operated pump at every station. Two samples of 2-4 L of unfiltered water were collected at each depth. Moreover, salinity was measured using a salinometer (YSI pro 600xl multiparametric probe) that was previously calibrated at each sampled depth. Sediment traps were deployed as explained below at every station and a CTD (Conductivity-Temperature-Depth) was deployed too. Furthermore, on February 1st sediment traps were recovered, and sediment cores were collected at each site.

Regarding the salinity, data measured by the salinometer was going to be used to define the salinity profiles as to derive the ^{238}U activity through its relationship with salinity (see section 3.3). However, due to calibration problems with the salinometer, it was decided to use the salinity data collected from the CTD. This decision was made after comparing the salinity data measured by the CTD and the salinometer at each station (i.e., M1, M2, M3 and M4). As a strong difference in salinity values was observed (salinometer > CTD), it was first decided to calculate the mean and standard deviation (i.e., 0.25) of the difference between methods to determine an error value and apply it to the original salinometer data (see Appendix, section 8.2). Although the correction made brought closer the values between the two instruments, the activity profiles from the different stations did not have a stable variation, therefore, it was decided to discard the salinometer data and use only the salinity data from the CTD. Besides, to validate the salinity data from the CTD, it was compared with salinity data registered from Universidad Politécnica de Cartagena (UPCT, 2024). The data used from UPCT represent the mean value from samples at different depths (from 0.5 to 5 m) and at least 12 diverse locations evenly distributed in Mar Menor (UPCT, 2024).

3.3. SAMPLE PROCESSING

On one hand, the sample processing for measuring ^{234}Th activity is divided in three different pathways as it was measured in seawater, sediment traps and core samples. Water and sediment traps samples were measured using a low-level beta Geiger-Müller multicounter, contrary to core samples which were measured by a well-type high-purity germanium detector as described below. On the other

hand, ^{238}U activity in seawater was derived from salinity following the relation salinity-uranium activity described by Owens et al. (2011).

3.3.1 Water

From the two water samples collected at each sampled depth (see section 3.2), one was processed for measuring particulate ^{234}Th and the other for measuring total (i.e., dissolved and particulate) ^{234}Th.

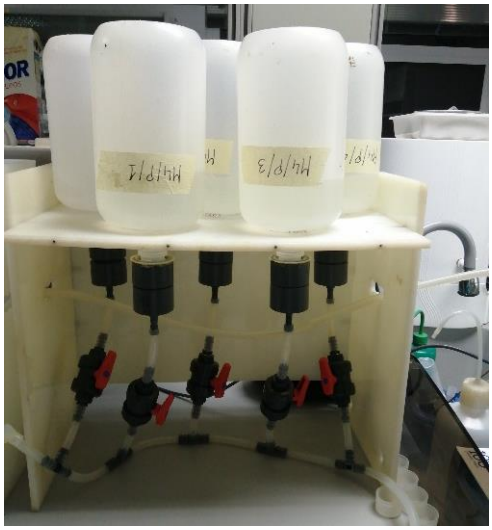

Figure 5. Picture of five samples being filtered onto the QMA filters at UPCT.

For particulate samples, no chemical treatment is needed so they were filtered shortly after collection in the laboratory at UPCT (Figure 5). Samples were filtered onto 25-mm diameter quartz microfiber filters (QMA). On the other hand, total samples were processed following the manganese dioxide (MnO_2) precipitation method described in Clevenger et al. (2021) and summarized in the protocol provided in Appendix, section 8.3. Briefly, first, samples were acidified using concentrated nitric acid (HNO_3) to a pH < 2. Next, working as the yield monitor, a known volume of ^{230}Th was added to each sample. After an equilibration time of at least 6 hours, sample's pH was raised to 8.0-8.5 by adding ammonium hydroxide (NH_4OH). This, along with the addition of potassium permanganate ($KMnO_4$) and manganese chloride ($MnCl_2$), allowed the formation of the MnO_2 precipitate. After a minimum of 8 hours, samples were filtered using QMA filters. After filtration, filter holders were rinsed with pH 9 water to minimize precipitate lost.

Once the filtration was completed, both particulate and total samples were then dried for 12 h. After that, dried samples were covered with one layer of mylar and two of aluminium foil to avoid the counting of low-energy beta emitters and measure ^{234}Th through the decay of its daughter, ^{234m}Pa ($T_{1/2}$ = 1.2 min), which is in secular equilibrium with ^{234}Th.

The radioactive decay of ^{234}Th produces the emission of a beta particle and gamma rays (Rodellas et al., 2023). Back at the UAB, water samples were counted using a low-level beta Geiger-Müller multicounter. In beta detectors, samples are let decay and as the emission of beta particles occurs a gas is pumped into the detector. The emission of these particles charges the molecules of the gas, which get ionized, and the electromagnetic field of the detector spot the pulse of charge. After about 1.5 months, all samples were recounted to estimate the activity from beta emitters other than ^{234}Th. This activity was subtracted from the first count. The activity of ^{234}Th at the time of collection was calculated by applying ingrowth and decay corrections and assuming chemical recoveries (which will be measured at least 5 months after sample collection, i.e., after July 2024). Nevertheless, due to technical and methodological issues some samples were lost (n = 4). Those were from M1 at 2 and 5 m deep; M2 at 6 m deep; and from M3 at 2 m deep.

3.3.2 Sediment traps

Eight sediment traps were used in total, with two traps at each station (Figure 6). Each pair of traps consisted of a about 8 m long rope attached to surface buoys on one edge and to a heavy weight on the other to keep the sediment traps in place. For particle collection, a metal structure with clamps was used to hold 6 glass test tubes of 13.40-15.30 mm diameter (Figure 7). Each test tube was placed in the clamps with the help of two rubber bands, trying to place them as vertically as possible so as not to spill sediment once filled. Each rope had 2 metal clamps: one placed at 1 meter above the bottom and the other at 3 meters.

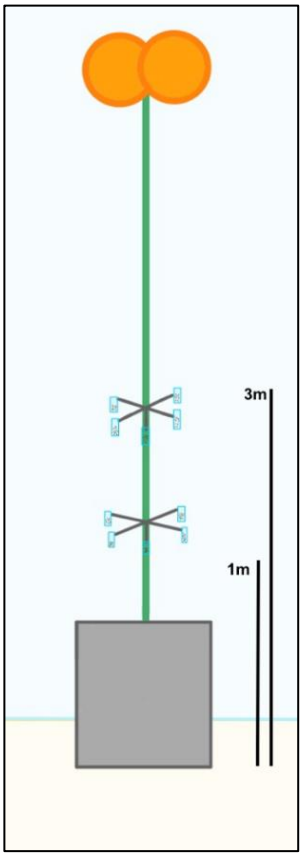

. *Figure 6. Schematic view of the assembling of each sediment trap. The grey rectangle symbolizes the weight, and the orange circles the surface buoys. There is one clamp at 1m above the bottom and the other one at 3 m, each one of them containing its respective test tubes.*

The operation of assembling the sediment traps was relatively simple. Metal brackets were first placed at the desired length of the rope and secured. The test tubes were then placed in the clamps and finally the rope was tied to the weight. Once the trap was assembled, the trap was deployed in the desired area, making sure that the tubes were vertically positioned for a good sample collection. Traps were recovered by divers a week later (6.9 days). The test tubes were capped in situ to avoid sample loss and then the traps were disassembled.

From each trap, the content of three test tubes was filtered onto a QMA filter, which was subsequently dried and weighed. Lastly, they were measured as water samples using the beta detector (see section 3.3.1).

It is important to note that due to windy weather (see section 4.1.1), sediment traps were left longer (almost 7 days) than planned in the first place (4 days). Furthermore, in location M1 the trap sediment at 1 m above the bottom was found completely at the bottom, and the trap placed at 3 m from the sediment bed, was found at 2 m above the bottom. Due to this, data from M1 trap found at the bottom, will not be considered and the distance from the bottom of the second one will be 2 m instead of 3 m.

Figure 7. Picture of the metal clamps with the 6 test tubes attached with plastic rubber bands.

3.3.3 Sediment: cores

Sediment cores were also collected to determine ^{234}Th activity in surface sediments. With the help of divers, one core from each location M1, M2, M3 and M4 was taken after the recovery of sediment traps. Cores used consisted of 1-m tubes that were penetrated in the sediment and then extracted. Once in the laboratory at UPCT, the upper 11 cm of each sediment core was sliced every 0.5-1.0 cm (Figure 8).

Once slices were properly cut, they were left drying in the stove at 60ºC for more than a week until there was no humidity. Once dry, the most superficial samples were homogenized. For this process,

samples were manually crushed in a mortar, removing before all the elements that were not the sediment itself, mainly the remains of algae and marine plants or shells. When all the sediment was fine-grained and homogenous, it was introduced into a vial and sealed with parafilm. In order to fill the vials, the top 0.5 cm samples from two consecutive depths were combined, i.e., sections 1-2 (from 0 to 1 cm) and 3-4 (from 1 to 2 cm).

The activity of ^{234}Th was measured by a gamma detector well-type high-purity germanium detector (HPGe). Germanium detectors are semiconductor detectors with two conduction bands and an intrinsic layer inside, which is sensitive to gamma rays. When this intrinsic layer detects the radiation, the electronic field formed between the two conduction bands produce an electric pulse that is then quantified (Mirion, 2024).

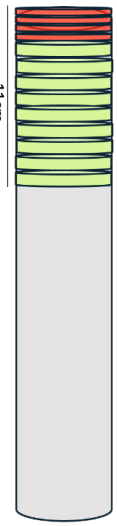

Figure 8. Drawing showing sections cut from the core. The first four red sections correspond to 0.5 cm slices from the first 2 cm of the cores. On the other hand, green sections correspond to remaining slices up to 11 cm deep cut every 1 cm.

4 RESULTS

4.1. PHYSICOCHEMICAL BACKGROUND

To properly contextualize and interpret results, physicochemical background information is needed. In this section, both meteorological and water column information taken from secondary sources and measured in the field are shown.

4.1.1 Meteorological and water column data

Physicochemical data from one month earlier than the campaign (i.e., December 25th of 2023) until the end of the campaign (i.e., February 2nd of 2024) is shown (Figure 9). Data shown in this section belong to two different sources: *Agencia Estatal de Meteorología* (AEMET) and UPCT. On the one hand, air temperature and wind speed data (Figure 9.A and B), which pertain to AEMET, are from the meteorological station *San Javier Aeropuerto*, at 4 m above sea level. On the other hand, water temperature, turbidity, salinity, transparency, oxygen and chlorophyll data (Figure 9.C, D, E, F, G and H), belonging to UPCT, represent a mean between different depths and locations along Mar Menor (see section 113.2).

On the one hand, during the month before sampling (December 25th to January 24th), air temperature, ranges from 2.1 to 21.6 ºC and has a mean of 12.4 ºC. On January 13th a decrease of the minimum temperature of approximately 8.0 ºC below average was registered (Figure 9.A). Wind speed ranges from 2.3 to 8.9 m s^{-1} with strikes reaching 24.2 m s^{-1} just six days before the first sampling (i.e., January 19th; Figure 9.B). Furthermore, water temperature ranges from 11.4 to 13.4 ºC and has a mean 12.4 ºC, like the average air temperature (Figure 9.C). Turbidity, which ranges from 0.4 to 1.5 FTU[5], shows quite constant values until January 16th when it starts increasing gradually and finally reaching 1.5 FTU two days before sampling (i.e., January 23rd, Figure 9.D). Salinity, which ranges from 42.6 to 44.1 PSU, has rather constant values until January 16th too, but contrary to turbidity, it decreases gradually reaching its minimum on January 23rd (Figure 9.E). Transparency does not show large variation as it ranges from -4.6 to -4.7 m (Figure 9.F), although, it slightly decreases through time. Oxygen, which ranges from 7.2 to 7.9 mg L^{-1}, predominantly shows a decreasing trend (Figure 9.G). Finally, chlorophyll, which ranges from 0.41 to 0.8 mg m^{-3}, shows noticeable variation, as it first increases until

[5] FTU: Formazine Turbidiy Unit

January 3rd, then gradually decreases until January 16th when it increases again until January 23rd (Figure 9.H).

On the other hand, during sampling (January 25th to February 1st), the average air temperature was 13.0 ºC, ranging from 5.8 to 24.0 ºC (Figure 9.A). The mean wind speed was 3.7 m s^{-1}, ranging from 1.7 to 6.4 m s^{-1}, but with strikes reaching 10.8 m s^{-1} (Figure 9.B). Water temperature, with a mean of 13.7 ºC (Figure 9.C); salinity, with a mean of 43.1 PSU (Figure 9.E); and oxygen, with a mean of 7.3 mg L^{-1} (Figure 9.G), show an increasing trend. While the increase in water temperature and oxygen is small, the difference in salinity is considerable, going from 42.8 to 43.4 PSU in seven days. At the same time, turbidity, with a mean of 1.2 FTU (Figure 9.D); transparency, with a mean of -4.7 m (Figure 9.F); and chlorophyll, with a mean of 0.59 mg L^{-1} (Figure 9.H), show a decreasing trend throughout the week. Turbidity and chlorophyll show a more accentuated decrease whereas the decrease in transparency is more gradual.

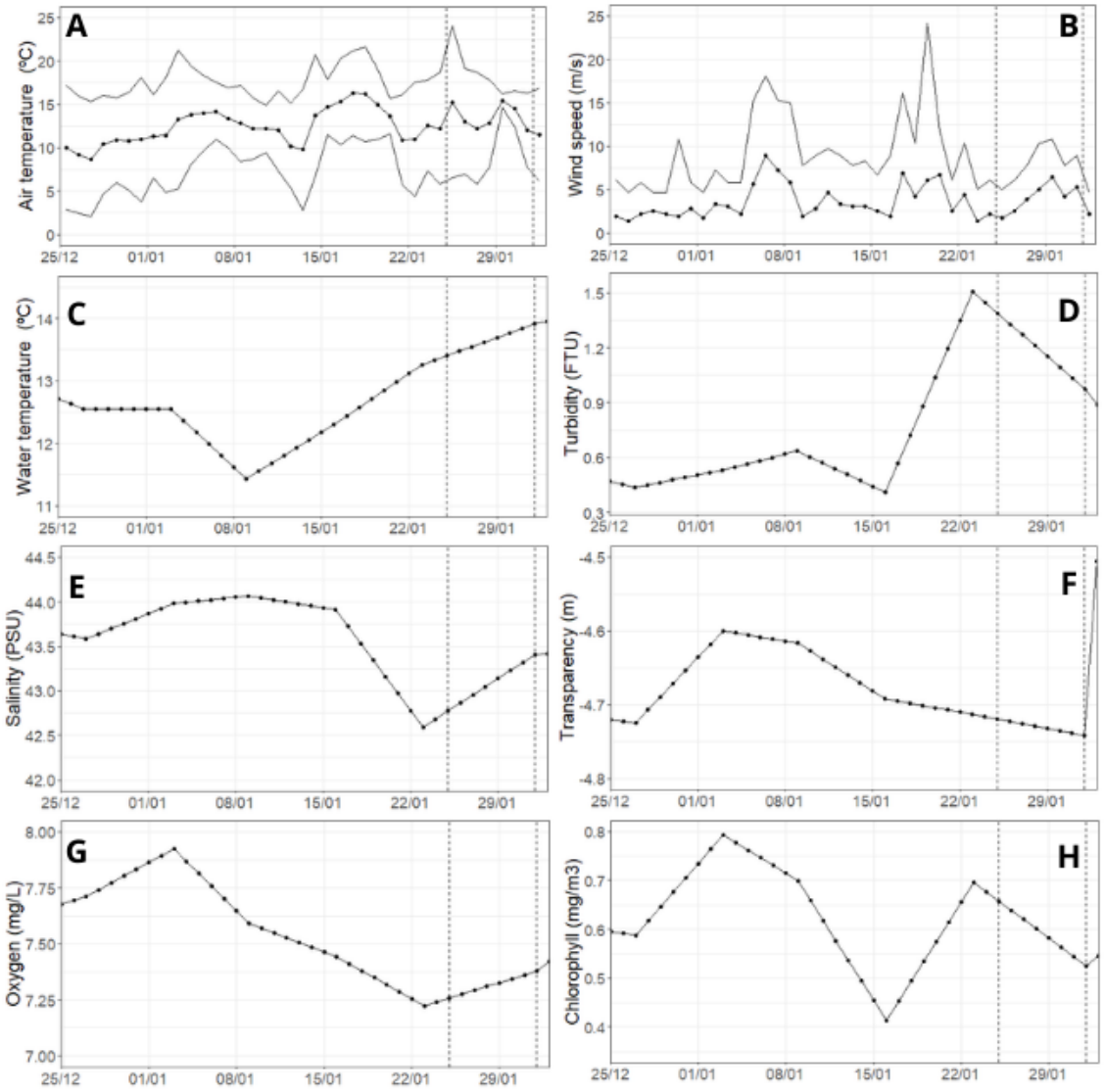

Figure 9. Physicochemical data one month earlier and during de campaign. A. Air temperature showing mean temperature with a black line with dots and the upper and lower lines correspond to the maximum and minimum temperatures, respectively; B. Average wind speed shown with a black line with dots and wind strikes speed shown with the upper line; C. Water temperature; D. Turbidity; E. Salinity; F. Transparency; G. Oxygen; H. Chlorophyll. Vertical dotted lines show 1. the date of collection of water samples and assembly of sediment traps, and 2. the date of collection of sediment traps and cores samples. Data of A and B from (AEMET, 2024); and the rest from (UPCT, 2024); all processed with (RStudio Team, 2020).

4.1.2 CTD *(Conductivity-Temperature-Depth)* sonde data

Furthermore, as explained in section 3.2, a CTD sonde was deployed in every station on January 25th. Temperature and salinity depth profiles are shown in Figure 10. On the one hand, the temperature in M2, M3 and M4 follows a decreasing trend with depth (more accentuated in M4), whereas the temperature in M1 increases with depth. The increase in surface water temperature observed from M1 to M4 is consistent with surface water warming during the day as the CTD was deployed firstly in M1, then in M2, followed by M3, and finally in M4 (> 3 hour-difference between M1 and M4; see Table 1, in Appendix, section 8.1).

On the other hand, regarding salinity, M1 station also follows a different trend compared with the other three, as salinity increases through depth, spanning from 43.1 to 43.6 PSU, and presents lower salinity values at all depths. On the contrary, in the two first meters in M2 and M4 salinity slowly decreases with a minimum of 43.9 PSU, but likewise in M3, salinity does not present considerable variation with depth (i.e., in M3 ranges from 44.1 to 44.2 PSU).

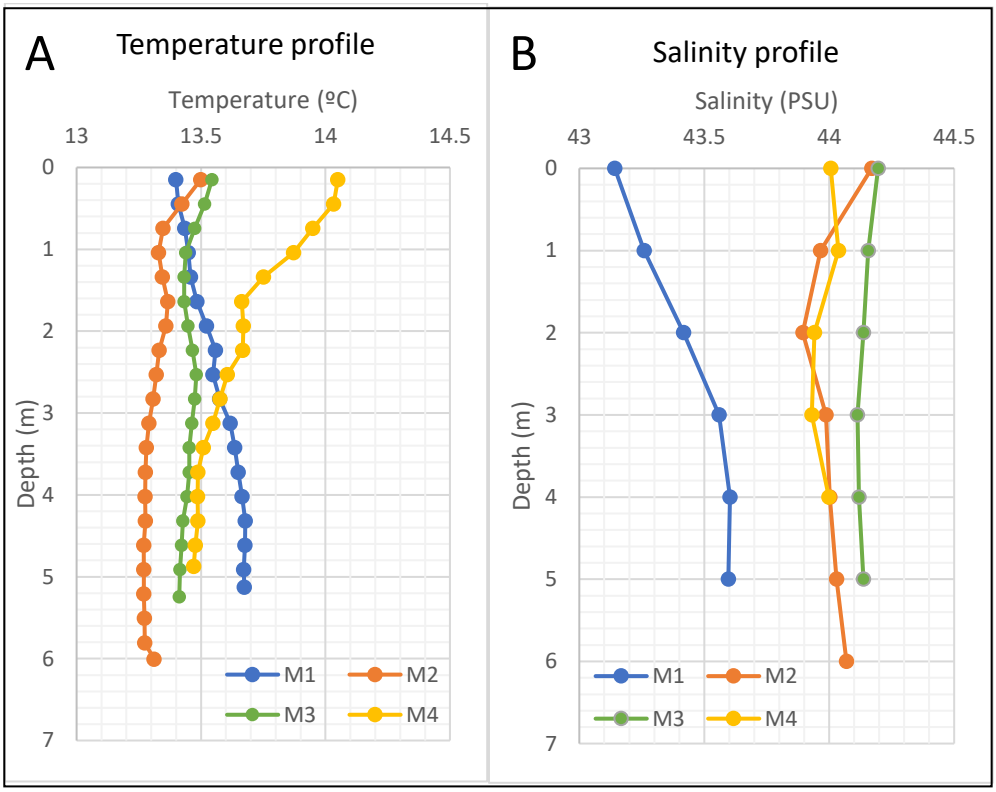

Figure 10. Temperature (A) and salinity (B) profile through depth in the different stations. Data shown from the Conductivity-Temperature-Depth (CTD) sonde.

4.2. ^{234}Th RESULTS

In this section, the results related to ^{234}Th are shown. As in section 3.3, this section is divided in water samples, for activity profiles of ^{234}Th and ^{238}U; sediment traps, for the flux of ^{234}Th and sedimentation rate; and finally cores for ^{234}Th activity in the bottom sediments.

4.3.1 Water

As mentioned in section 3.3.1, two types of samples were collected for water: particulate and total. However, the particulate fraction represents an average of 28% of the total: in M1, 11 ± 9 %; in M2, 21 ± 7 %; in M3, 24 ± 13 %; and in M4, 56 ± 13 % (average ± standard deviation). Given the low activity

of particulate samples, they have high uncertainties. For that reason, these samples have not been used and all water results correspond to total samples. Nevertheless, it is worth emphasizing that M4 shows higher contributions of particulate ^{234}Th activities, reaching 74% at 2 m deep. Furthermore, at a few meters deep (i.e., 2 and 3 m), in all the stations, more particulate ^{234}Th activity is measured than in shallow (i.e., 0 and 1 m) or deeper waters (i.e., ≥ 4 m) (see Table 2 in Appendix, section 8.1).

Figure 11 shows the activity profiles of ^{234}Th and ^{238}U in each of the sampling locations. ^{234}Th activity minimum is located at 2 m deep in station M4 with a value of 0.31 ± 0.13 dpm L^{-1}, while the maximum 0.72 ± 0.10 dpm L^{-1}, appears at 4 m deep in station M1. There is an overall ^{234}Th activity mean of 0.47 ± 0.11 dpm L^{-1} considering all stations. All stations except M1 do not show considerable variation in ^{234}Th activity through depth. ^{234}Th activity in M2 and M4 stations remains mostly constant, whereas in M3 it shows a little increase (Figure 11.C). However, ^{234}Th activity in M1 increases from 0.46 ± 0.09 dpm L^{-1} to 0.72 ± 0.10 dpm L^{-1}.

^{238}U activities are very similar with depth and across stations with an average activity of 3.14 ± 0.02 dpm L^{-1}. ^{234}Th activities are always lower than ^{238}U activities throughout the water column in all four sampling stations, and the difference between ^{234}Th and ^{238}U activity profiles presents general similarities across stations. Considering all four stations, there is an overall mean difference between the activity of ^{234}Th and ^{238}U of 2.67 ± 0.11 dpm L^{-1}.

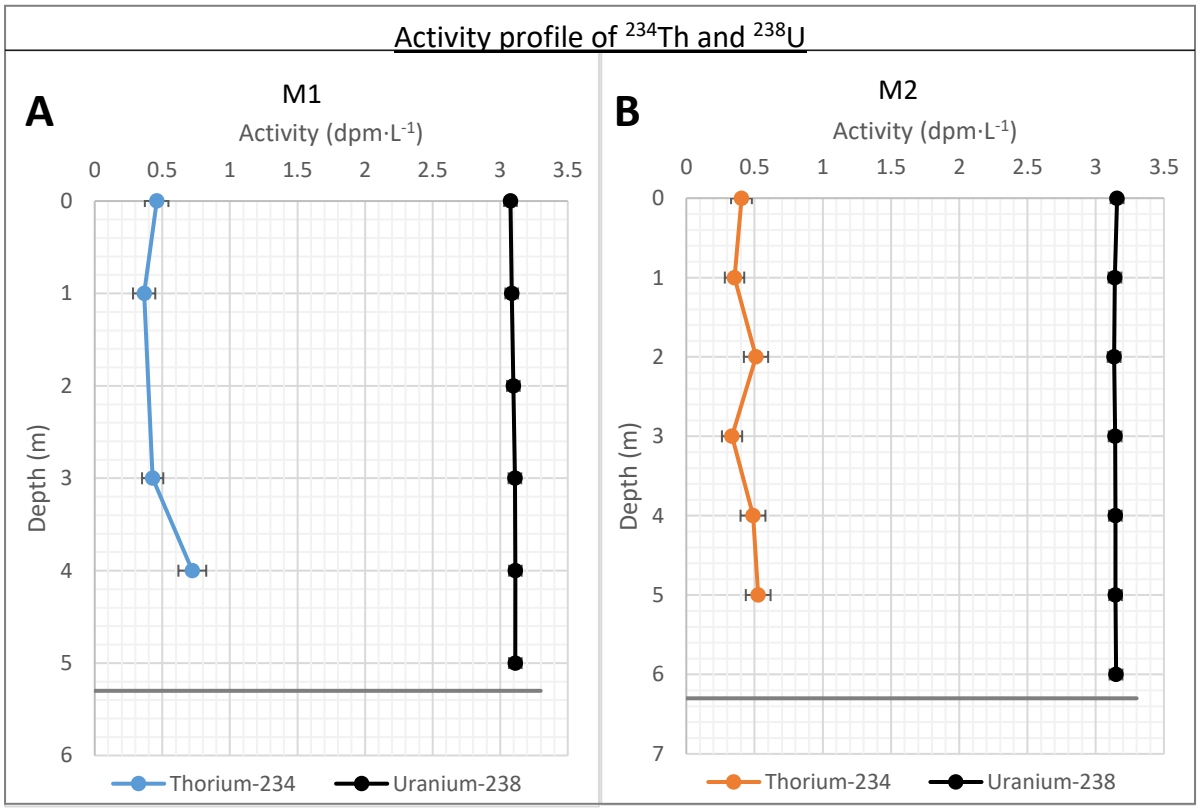

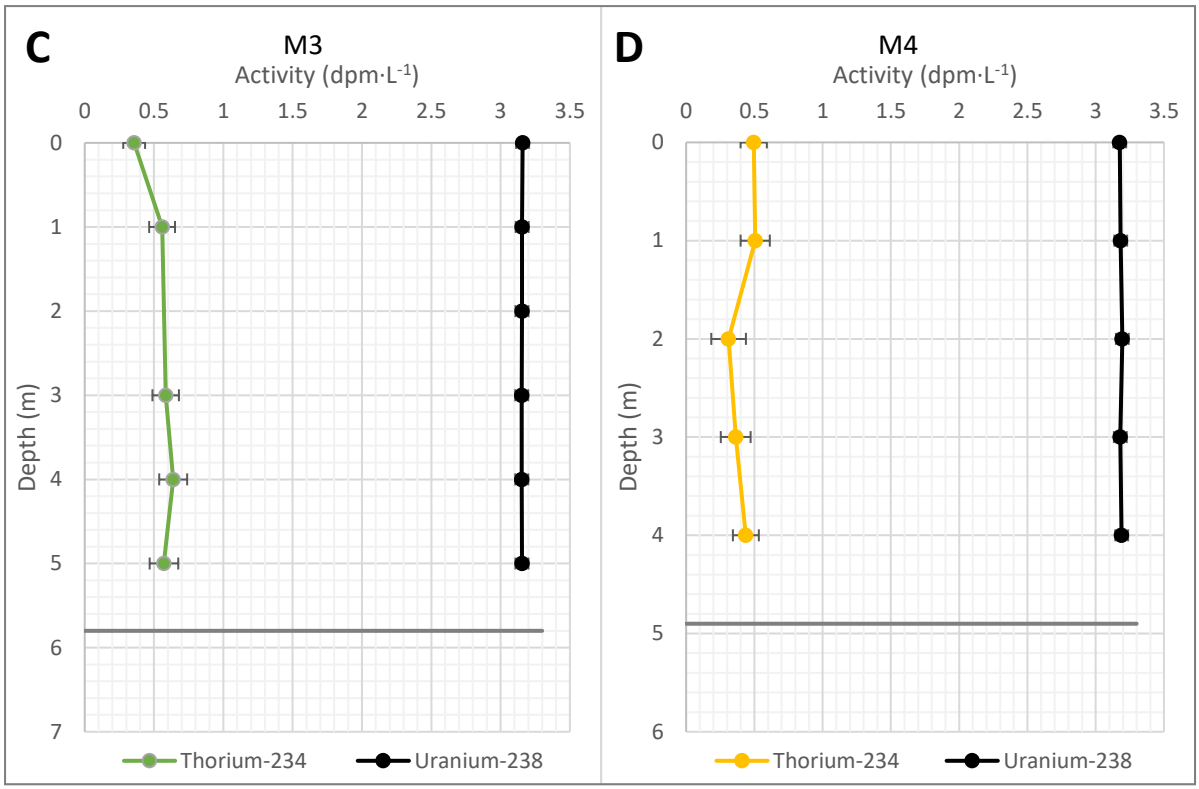

Figure 11. Activity profiles of ^{234}Th and ^{238}U in A. M1 station, B. M2 station, C. M3 station and D. M4 station. Gray lines represent the depth of the bed sediment.

4.3.2 Sediment traps

In this section, the flux of ^{234}Th and sedimentation rates from sediment traps are shown. These results show greater variation across stations and depths than the activity profiles of ^{234}Th and ^{238}U from water samples. Regarding the flux of ^{234}Th, two stations, M2 and M4 show an increasing trend with depth (Figure 12.A), whereas M3 does not show a change with depth. Moreover, ^{234}Th flux from M1, M2 and M3 close to 3 m depth is about 100 dpm m^{-2} d^{-1} (i.e., 113 ± 23, 95 ± 27 and 102 ± 27 dpm m^{-2} d^{-1}, respectively), yet M4 reaches more than 350 dpm m^{-2} d^{-1} close to 4 m depth (i.e., 374 ± 52 dpm m^{-2} d^{-1}; Figure 12.A). Furthermore, a large difference is seen between M4 and the other stations regarding sedimentation rates, with rates from 6.8 to 8.4 g m^{-2} d^{-1} in M4 compared to rates from 3.3 to 3.7 g m^{-2} d^{-1} in M1, M2 and M3. Also, M3 and M4 stations show a decrease in sedimentation rates throughout depth, whereas M2 does not (Figure 12.B).

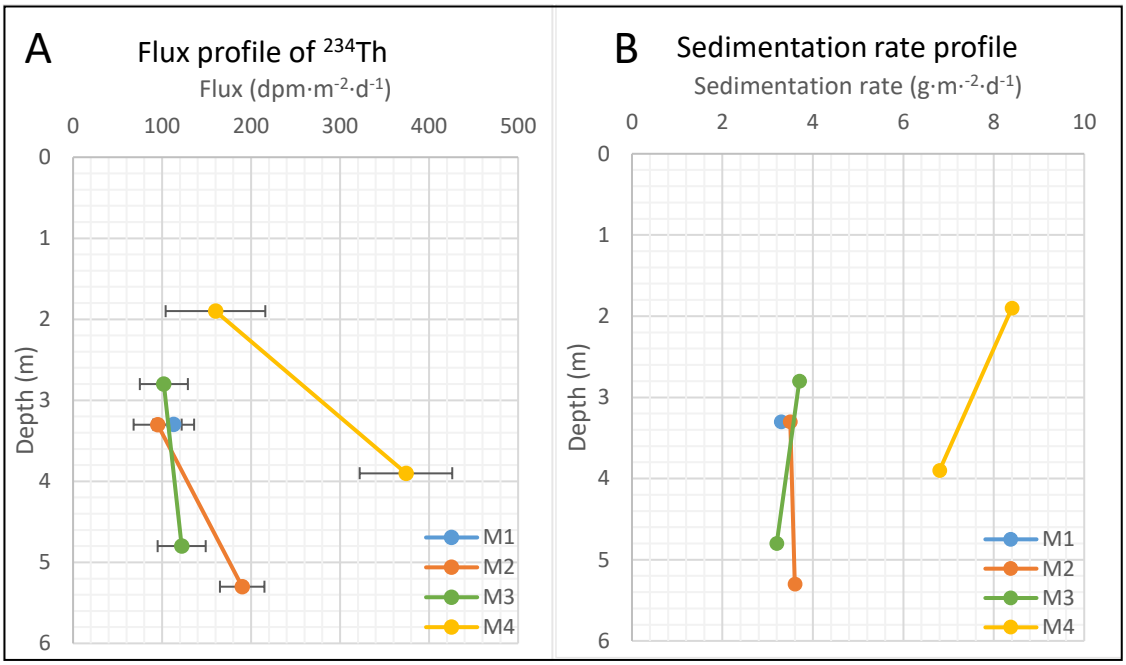

Figure 12. Flux profile of ^{234}Th (A) and sedimentation rate profile (B) from sediment traps in the different stations. Error bars show uncertainty.

4.3.3 Sediment: cores

Sediment cores taken at the bottom of the lagoon show variation in ^{234}Th activity with depth in M2 and M3 stations, contrary to M1 and M4 (Figure 13). From the first sediment layer (0-1 cm) to the second layer (1-2 cm) a decreasing trend in ^{234}Th activity is observed in M2 and M3, going from 67.9 ± 7.6 and 58.7 ± 10.2 Bq kg^{-1}, to 33.0 ± 2.4 and 28.7 ± 2.4 Bq kg^{-1}, respectively. Nevertheless, considering uncertainties, no variation in ^{234}Th activity is observed from the second to the third layer (2-3 cm) in any station. Furthermore, in the first sediment layer, the ^{234}Th activity for M1 is 49.2 ± 0.1 Bq kg^{-1} and for M4 is 23.0 ± 11.2 Bq kg^{-1}, the latter showing the lowest activities of all four stations.

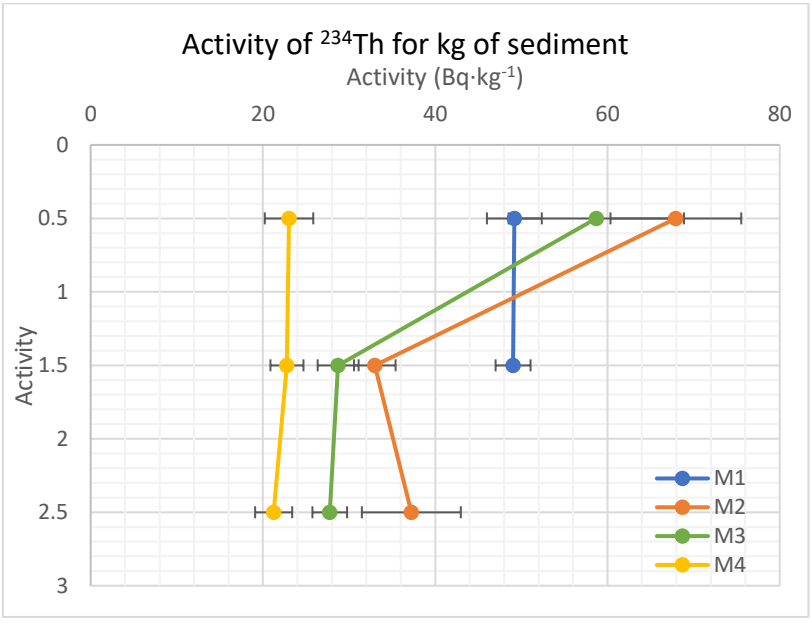

Figure 13. ^{234}Th activity in a kg of sediment in cores samples in the different stations. The 0.5 datapoint refers to the ^{234}Th activity from 0 to 1 cm of sediment; 1.5, from 1 to 2 cm; and 2.5, from 2 to 3 cm. Error bars show uncertainties.

5 DISCUSSION

5.1. ^{238}U-^{234}TH ACTIVITY WATER PROFILES ANALYSIS

^{238}U and ^{234}Th activity depth profiles shown in this study differ from the usual activities of these isotopes in the open ocean (Ceballos-Romero et al., 2022) or shallower waters like the study from a coastal semi-restricted lagoon conducted by Black et al. (2023). While in the open ocean ^{234}Th activity is around 2 dpm L^{-1} (Ceballos-Romero et al., 2022), in Mar Menor the ^{234}Th activity measured in the water column was four times lower (0.47 ± 0.11 dpm L^{-1}). Furthermore, Black et al. (2023) found activities of 0.90 ± 0.20 dpm L^{-1}, which are also lower than those reported in the open ocean, yet more similar to Mar Menor's. ^{238}U activity found in the open ocean is around 2.40 dpm L^{-1} (Owens et al., 2011) under a mean salinity of 35 PSU (NOAA, 2023). In comparison, at the coastal study site in Black et al. (2023), ^{238}U activities ranged from 2.02 dpm L^{-1} to 2.14 dpm L^{-1} and salinities from 29.7 to 31.3 PSU. In the hypersaline lagoon of Mar Menor, derived ^{238}U showed an average activity of 3.14 ± 0.02 dpm L^{-1} and measured salinity ranged from 43.1 to 44.2 PSU.

The disequilibrium found between the two radioisotopes translates as a ^{234}Th activity deficit (i.e., ^{238}U-^{234}Th activity). As explained in section 1, as ^{234}Th is highly particle-reactive, in the presence of particles, it is adsorbed onto them and removed from the water column associated with particle export, while ^{238}U remains in the water column. This produces a ^{234}Th activity deficit that is commonly seen in the upper water column because of primary production and subsequent export of sinking particles, but that can also be observed near the seabed by particle resuspension (Figure 1). In Mar Menor larger ^{234}Th deficits in the water column than those typically observed in the open ocean or in Black's study were found. Those deficits could be related to a higher particle concentration and consequently, a more reactive surface for ^{234}Th adsorption in the whole water column, favouring the export of ^{234}Th associated with the movement of particles in the lagoon (i.e., particles exported vertically or laterally). In open oceans, there is a clear difference between the isotope's activities usually throughout the first 100 m, where, at that point, they reach the secular equilibrium, indicating no further net removal of ^{234}Th associated with sinking particles (see Figure 1.A, Rodellas et al., 2023). However, the ^{234}Th deficit found in Mar Menor, as in the study conducted by Black et al. (2023), is observed throughout the entire water column. As both studies were conducted in coastal shallow waters, a higher particle concentration and therefore greater export and deficit of ^{234}Th, are expected. Nevertheless, Black et al. (2023) found a higher difference between the activities of ^{238}U and ^{234}Th in the first meters of the water column (upper 10 m), followed by an increase in ^{234}Th activities at mid-depths (between 10 and 40 m), and a slight decrease in ^{234}Th activity near the seabed as expected in Figure 1.B, that could be potentially related with resuspension. On the contrary, the ^{234}Th activity depth profile found in this study did not follow this trend since it was vertically constant along the water column.

To better understand the ^{234}Th deficits observed in the water column, it is important to consider the timescale they represent. Given the half-life of ^{234}Th ($T_{1/2}$ = 24.1 days), the water column ^{234}Th data integrates particle processes that occurred during about a month prior to sampling, i.e., approximately from December 25th to January 25th. The vertical ^{234}Th activity trend in the water column seen in this study could be related to high particle concentration along all the water column (enhancing the adsorption of ^{234}Th on particles), as well as both horizontal and vertical export of particles carrying ^{234}Th. As described in section 4.1.1, after strong wind strikes (>20 m s^{-1}) turbidity and chlorophyll concentration increased two days before sampling (i.e., January 23rd). The strong wind strikes reaching the shallow waters could have induced a mix of the water layers as described in García & Muñoz-Vera (2015). The Mar Menor lagoon is affected by several currents (Díaz del Río & Somoza Losada, 1993) which can be divided into two water layers: one superficial at 0.7-3.0 m deep and a deeper one until

the sediment bed (Ruiz et al., 2020). The mean speed at the water column can also be divided in two, where at the surface layer of the water column is about 2.5 cm s^{-1}, while the deeper water layer has a higher speed of 2.9 cm s^{-1} (Ruiz et al., 2020). However, if there are high-speed winds, the dynamics of the lagoon can locally change, merging the top and bottom layers, creating high turbidity areas due to the flocculation of the particles (García & Muñoz-Vera, 2015). Thus, this effect ends up modifying the possible particle fluxes. These circumstances occur since the setting of fine-grained sediments is enhanced by the mixing of salt concentration water and stressed by the wind and the shallow waters. For that reason, if there are high-speed winds, even with the slightest increase in salinity can favour flocculation, which is the process of the aggregation of fine clay particles (García & Muñoz-Vera, 2015). Moreover, the aggregation of the fine particle implies an increase in the grain size and its sedimentation speed. This hypothesis is supported with turbidity and chlorophyll data from January 23rd (UPCT, 2024) showing high values, in mostly all the water column for turbidity (see Figure 15 and Figure 16 in Appendix, section 8.4) contrary to the other days studied. Moreover, the difference seen between Black et al. (2023) study and this one on ^{234}Th deficit along the water column, could be due to the different depths in the water column of 70 m and 5 m, respectively, as in shallower waters meteorological phenomena (like seen here wind) could favour the mixing of all the water column. The mixing of the water layers could play a big role in resuspension which in turn could contribute on enhancing the flocculation and thus the increased turbidity episode. However, in this study, due to a lack of data to compare, no conclusive evidence is found.

5.2. ^{234}TH FLUXES AND SEDIMENTATION RATES

In relation to sediment traps results, the timescale they represent is different from the water column. While water samples reflect the physicochemical background from the month prior to sampling, as the effect of some parameters (i.e, turbidity or wind speed) remain noticeable for longer in the water column, sediment traps only record data during the time they are actively collecting samples. Therefore, sediment traps show only results from the week they were collecting particles, i.e., from January 25th to February 1st while water samples show information from December 25th to January 25th.

Furthermore, to be able to compare the ^{234}Th results from the water column and sediment traps, it is important to determine the ^{234}Th fluxes derived from the deficits observed in the water column. To do this, the method described by Rodellas et al. (2023) was followed, integrating the measured ^{234}Th deficits throughout the entire water column and considering the ^{234}Th decay constant (λ_{Th} = 0.02876 day^{-1}). This method is needed to transform ^{234}Th activity deficits onto ^{234}Th fluxes to compare the different type of samples (assuming 1-dimensional steady-state conditions; Rodellas et al. 2023).

As previously explained in section 4.3.2, sediment trap data show big differences in sedimentation rates and ^{234}Th fluxes between stations, as M4 doubles M1, M2 and M3 values in both parameters (Figure 12.B). However, the ^{234}Th flux derived from water samples (see Table 3, Appendix, section 8.5) is similar in all four stations: M1 = 394 dpm m^{-2} d^{-1}, M2 = 488 dpm m^{-2} d^{-1}, M3 = 432 dpm m^{-2} d^{-1} and M4 = 384 dpm m^{-2} d^{-1} (see Table 3 in Appendix, section 8.5). This inconsistency among results could be explained because of the differences between timescales tracked by water and sediment trap samples: water samples give information about ^{234}Th fluxes during one month before sampling, whereas sediment trap samples give information on ^{234}Th fluxes during a week after the water sampling.

There are temporal inconsistencies when trying to relate and give conclusions. However, the difference between results could be supported by high turbulence values detected on February 1st at

the bottom layer of the water column in the westernmost area of Mar Menor (where M4 is located; see Figure 17 in Appendix section 8.4). As a result of the increased turbidity, more particles in the water column were depositing on the sediment bed and the sediment traps from M4 station recorded that phenomenon. Furthermore, sedimentation rates from other studies have also been considered to contextualize the results from this study. A prior study carried out in Mar Menor has also found higher sedimentation rates around station M4 (I. Alorda, pers. comm). This finding has been related to its location near the mouth of *El Albujón* stream, which provides tons of sediments daily (Marco et al., 2016).

5.3. Further evidence for particle fluxes in Mar Menor from sediment cores

Like water samples, the temporal window of sediment cores covers about a month prior to sampling. Therefore, sediment cores in this study reflect ^{234}Th sedimentation processes approximately from January 1st to February 1st.

As previously described in section 4.3.3, two main different features in sediment cores are observed (Figure 13). While in M1 and M4 stations ^{234}Th activity remains constant through sediment depth, M2 and M3 show a different trend. Those two stations (i.e., M2 and M3) record higher values in the first centimetre (i.e., 0-1 cm) with a later decrease on the second centimetre (i.e., 1-2 cm), where then ^{234}Th activity remains constant (i.e., 2-3 cm). The vertical constant trend implies that all ^{234}Th activity measured comes from ^{238}U disintegration (or supported ^{234}Th), thus there is not any further ^{234}Th supply rather than the supported one. Consequently, in the first centimetre of M2 and M3, where this vertical trend is not recorded, another supply of ^{234}Th is noticed besides the supported one. This could mean that this additional supply of ^{234}Th measured comes from the water column above. However, ^{234}Th activity profiles (Figure 11) show almost the same ^{234}Th activity in all samples and no considerable difference is noticed along the stations. Hence, if the activities are similar along the stations, horizontal flux needs to be considered as the additional supply of ^{234}Th on the sediment bed in M2 and M3 stations.

The different activities in M4 station in relation with the other three stations could be due to its location near *El Albujón* stream, an area that suffers from strong drag or entrainment processes (near Sampling Station 1 or SS1, in García & Muñoz-Vera, 2015), and therefore creates a horizontal particle flux that drags the possible sedimentation away from this area. In contrast, M2 station (as SS3, in García & Muñoz-Vera, 2015) is located at the north-centre area of the lagoon which, due to the same currents, concentrates high quantities of sediment in comparison to M4. The same phenomena could be happening as well in M3 as it is also at the centre of one of the cyclonic gyres. M1, however, is in the northern anticyclonic cell (Ruiz et al., 2020) where both sedimentation and entrainment processes occur (García & Muñoz-Vera, 2015).

Nevertheless, comparing the ^{234}Th activity value from cores and sediment traps samples, we would expect in M4 a higher activity on the surface of the core due to a higher sedimentation rate (Figure 12) at the sediment trap. Moreover, the timescale covered by core samples includes both the one covered by sediment trap samples and a part of the one covered by seawater samples. That is why, inconsistencies seen in this case should not be related with timescale but with physical processes affecting the lagoon and its particle dynamics. Consequently, the lack of an increased ^{234}Th activity in M4 could be related with a slow particle deposition rate as cores and sediment trap samples were taken the same day turbidity increased (i.e., February 1st, see section 5.3).

These described processes help to put together the different pieces of information provided by each sample type. Taken together, to our understanding, although the lagoon of Mar Menor may appear to be a stagnant area due to geography, it is defined by a large number of interconnected processes that aid in the mobilization of particles within it.

5.4. LIMITATIONS AND INSIGHTS FOR FUTURE RESEARCH

This study is the first in this field to be conducted in Mar Menor. The $^{234}Th/^{238}U$ pair has been historically used to determine particle fluxes and track POC from the surface to the deep ocean, but its use in coastal systems is very limited (García & Muñoz-Vera, 2015). Therefore, as this is a leading study, while developing the sampling campaign and analysing data and results, it has been noticed that some procedures could be improved in future studies.

In the first place, in this study, only one sampling campaign was carried out. Besides, there were not any previous ^{234}Th data from Mar Menor as it is an innovative path of research. This fact complicates the interpretation of results, as there is no data to compare to. Furthermore, we suggest that the sampling should be repeated on different environmental conditions to corroborate our conclusions. For instance, there is no knowledge if the increased turbidity events always induce the mixing of the water layers and cause a vertical ^{234}Th activity profile or if it is caused by another phenomenon. Besides, in this study, sediment trap samples had to be deployed following water sampling which led to a temporal inconsistency. To minimize this, it is recommended to deploy sediment traps first and collect seawater samples and sediment cores when recovering the sediment traps. Therefore, water and cores should be taken when sediment traps have already collected the samples

To improve the resolution of ^{234}Th activity in the water column profiles, water samples should be taken every 0.5 m instead of 1 m. Thus, the distribution of the ^{234}Th activity throughout the water column could be described in more detail and samples closer to the bottom could be taken. This high-resolution sampling will be helpful to elucidate whether ^{234}Th can be a suitable tracer for resuspension in Mar Menor.

Furthermore, the relation used to determine ^{238}U activity from salinity, from Owens et al. (2011), was obtained from salinities between 32.7 to 37.1 PSU, whilst salinities in Mar Menor are considerably higher. However, other relationships covering larger salinity ranges were compared (i.e., Pates & Muir, 2007 and Not et al., 2012) to Owens et al. (2011) and the differences were very little (i.e., 0.2 % between Owens et al. 2011 and Pates & Muir 2007, and 5.0% from Not et al., 2012). To prevent errors for future research and to confirm the ^{238}U activities derived, we recommend taking water samples in order to analyse ^{238}U.

It is important to note that this study is a breakthrough in the use of $^{234}Th/^{238}U$ technique and an open window to related future research in Mar Menor and other coastal areas. Taking the considerations exposed in this section, this methodology could be used to help understand better particle dynamics in shallower waters.

Finally, it is essential to highlight the importance of fixed stations that collect data continuously. Thanks to long-term meteorological and physicochemical data collected by the UPCT in different stations from the lagoon, we have been able to contextualize our results and make further hypothesis on which processes could have influenced our findings.

6 CONCLUSIONS

This was the first $^{234}Th/^{238}U$ study carried out with the purpose of studying particle dynamics in Mar Menor and assessing whether ^{234}Th can be a suitable tracer for resuspension in this coastal system. Our findings suggest evidence for both vertical and horizontal particle fluxes. Nevertheless, no clear sign of resuspension was found.

The main observations of this study are:

- Firstly, water samples recorded lower ^{234}Th activity than in open oceans and in Black et al. (2023) coastal study yet more similar to Black's et al. (2023). Moreover, contrary to our hypothesis (Figure 1.B), our ^{234}Th activity depth profile had a vertical constant trend along the column, unlike the first study which had more ^{234}Th deficit on the first meters deep and near the seabed. These findings could be due to high-speed winds two days before taking water samples (i.e., January 23rd) which mixed the water layers, easing the flocculation of particles and resulting on a high turbidity episode (García & Muñoz-Vera, 2015). And therefore, modifying the possible particle fluxes and enhancing resuspension.
- Secondly, contrary to water samples, sediment trap samples differ along the different stations. The three first stations (i.e., M1, M2 and M3) had lower ^{234}Th flux and sedimentation rate than M4 station. These results could be explained by a high turbidity episode near M4 on February 1st, when sediment samples were taken (both traps and samples), which eventually translated on high values on the sedimentation rates recorded by the sediment traps.
- Thirdly, like sediment trap samples, core samples activity results were different along the different stations. By contextualising the physicochemical background, it was found that M4 is located near the mouth of *El Albujón* stream in an area known by its dragging processes. This fact makes the sedimentation very difficult in M4, contrary to M2 that is located at the centre of the cyclonic gyre, where is common the sedimentation processes. Furthermore, M2 and M3 stations, had the highest ^{234}Th activity in the first centimetre of sediment and a later decrease of activity through depth suggesting an external supply of ^{234}Th besides the supported one. And, considering the vertical trend of the water samples, this additional supply could come from a horizontal flux.
- Lastly, core sample results seem to have a different trend from sediment trap samples, however, the disparity could be due to temporal inconsistencies, as core and water samples record data from one month before the sampling (i.e., core samples from January 1st to February 1st and water samples from December 25th to January 25th) and traps only during the time they are set (i.e., from January 25th to February 1st). And, although the temporal window of cores and sediment trap samples concur, the lack of an increased ^{234}Th activity in M4 could be due to a slow deposition of the particles as these samples were taken on the same day of the episode of increased turbidity of February 1st.

The $^{234}Th/^{238}U$ pair has been used for many decades to trace particle fluxes in the deep ocean, but its potential should be used in other systems, such as coastal areas like Mar Menor lagoon. Here, as a novelty, the radionuclide pair is used on a very shallow water column of 5 m deep. To assess whether ^{234}Th could work as a particle tracer in shallow waters like Mar Menor's, different types of samples were taken (i.e., water, sediment trap and core samples) as well as high-frequency physicochemical data in order to make consistent conclusions.

Ultimately, the recommendations outlined in this study will be helpful for future research to elucidate whether ^{234}Th can be used as a tracer for resuspension and to provide more knowledge about the environmental implications of resuspension affecting the fragile ecosystems living in Mar Menor.

7 REFERENCES

AEMET. (2024). *Agencia Estatal de Meteorología: Datos climatológicos*. https://www.aemet.es/es/serviciosclimaticos/datosclimatologicos

Aller, R. C., & Cochran, J. K. (1976). ^{234}Th/ ^{238}U disequilibrium in near-shore sediment: Particle reworking and diagenetic time scales. *Earth and Planetary Science Letters*, *29*(1), 37–50. https://doi.org/10.1016/0012-821X(76)90024-8

Amaral, V. J., Lam, P. J., Marchal, O., Roca-Martí, M., Fox, J., & Nelson, N. B. (2022). Particle cycling rates at Station P as estimated from the inversion of POC concentration data. *Elementa: Science of the Anthropocene*, *10*(1), 1415–1428. https://doi.org/10.1525/ELEMENTA.2021.00018

Azuara, J., Lebreton, V., Dezileau, L., Pérez Ruzafa, A., & Combourieu-Nebout, N. (2020). Middle and Late Holocene vegetation history of the Murcia region from a new high-resolution pollen sequence from the Mar Menor lagoon. *Journal of Archaeological Science: Reports*, *31*, 102–353. https://doi.org/10.1016/j.jasrep.2020.102353

Bhat, S. G., Krishnaswamy, S., Lal, D., Rama, & Moore, W. S. (1969). ^{234}Th/ ^{238}U Ratios in the oceans. *Éarth and Planetary Science Letters*, 483–491.

Black, E. E., Algar, C. K., Armstrong, M., & Kienast, S. S. (2023). Insights into constraining coastal carbon export from radioisotopes. *Frontiers in Marine Science*, *10*, 1254316. https://doi.org/10.3389/FMARS.2023.1254316/BIBTEX

Black, E. E., Anderson, R. F., Fleisher, M. Q., Holmes, K., Kienast, S., Weber, T. S., & Xu, H. (2024, February 22). *The Complexities of Constraining Carbon Export in Coastal Zones: Insights From Radioisotopes in Two North Atlantic Basins*. https://agu.confex.com/agu/OSM24/meetingapp.cgi/Paper/1491080

Boyd, P. W., Claustre, H., Levy, M., Siegel, D. A., & Weber, T. (2019). Multi-faceted particle pumps drive carbon sequestration in the ocean. In *Nature* (Vol. 568, Issue 7752, pp. 327–335). Nature Publishing Group. https://doi.org/10.1038/s41586-019-1098-2

Buesseler, K. O., Benitez-Nelson, C. R., Moran, S. B., Burd, A., Charette, M., Cochran, J. K., Coppola, L., Fisher, N. S., Fowler, S. W., Gardner, W. D., Guo, L. D., Gustafsson, Ö., Lamborg, C., Masque, P., Miquel, J. C., Passow, U., Santschi, P. H., Savoye, N., Stewart, G., & Trull, T. (2006). An assessment of particulate organic carbon to thorium- ^{234} ratios in the ocean and their impact on the application of ^{234}Th as a POC flux proxy. *Marine Chemistry*, *100*(3-4 SPEC. ISS.), 213–233. https://doi.org/10.1016/j.marchem.2005.10.013

Buesseler, K. O., Boyd, P. W., Black, E. E., Siegel, D. A., Designed, D. A. S., & Performed, E. E. B. (2020). Metrics that matter for assessing the ocean biological carbon pump. *Perspective*. https://doi.org/10.1073/pnas.1918114117/-/DCSupplemental

Caballero Pedraza, A., Romero Díaz, A., & Espinosa Soto, I. (2015). Cambios paisajísticos y efectos medioambientales debidos a la agricultura intensiva en la Comarca de Campo de Cartagena-Mar Menor (Murcia). In *Estudios Geograficos* (Vol. 76, Issue 279, pp. 473–498). CSIC Consejo Superior de Investigaciones Cientificas. https://doi.org/10.3989/estgeogr.201517

Ceballos-Romero, E., Buesseler, K. O., & Villa-Alfageme, M. (2022). Revisiting five decades of ^{234}Th data: a comprehensive global oceanic compilation. *Earth System Science Data*, *14*(6), 2639–2679. https://doi.org/10.5194/essd-14-2639-2022

Clevenger, S. J., Benitez-Nelson, C. R., Drysdale, J., Pike, S., Puigcorbé, V., & Buesseler, K. O. (2021). Review of the analysis of ^{234}Th in small volume (2–4 L) seawater samples: improvements and recommendations. In *Journal of Radioanalytical and Nuclear Chemistry* (Vol. 329, Issue 1). Springer Science and Business Media B.V. https://doi.org/10.1007/s10967-021-07772-2

Cochran, J. K., Barnes, C., Achman, D., & Hirschberg, D. J. (1995). Thorium-234/uranium-238 disequilibrium as an indicator of scavenging rates and particulate organic carbon fluxes in the Northeast Water Polynya, Greenland. *Journal of Geophysical Research*, *100*(C3), 4399–4410. https://doi.org/10.1029/94JC01954

Cochran, J. K., & Masqué, P. (2003). Short-lived U/Th Series Radionuclides in the Ocean: Tracers for Scavenging Rates, Export Fluxes and Particle Dynamics. In *Applications of Short-lived Radionuclides in the Ocean* (pp. 461–492).

Conesa, H. M., & Jiménez-Cárceles, F. J. (2007). The Mar Menor lagoon (SE Spain): A singular natural ecosystem threatened by human activities. *Marine Pollution Bulletin*, *54*(7), 839–849. https://doi.org/10.1016/j.marpolbul.2007.05.007

De La Rocha, C. L., & Passow, U. (2014). The Biological Pump. *Treatise on Geochemistry: Second Edition*, *8*, 93–122. https://doi.org/10.1016/B978-0-08-095975-7.00604-5

Díaz del Río, V., & Somoza Losada, L. (1993). Mapa fisiográfico del Mar Menor. *Instituto Español de Oceanografía*, *Publ. Especiales 14*.

Fernández, J. M., & Esteve Selma, M. A. (2007). Gestión integrada de cuencas costeras: dinámica de los nutrientes en la cuenca del Mar Menor (sudeste de España). *Dinámica de Sistemas*, *3*(1).

Fernández, J. M., Fitz, C., Selma, M. A. E., Guaita, N., & Martínez-López, J. (2013). Modelling the effects of land use change on the nutrient dynamics in a coastal agricultural watershed: The Mar Menor case (Southeastern Spain). *Ecosistemas*, *22*(3), 84–994. https://doi.org/10.7818/ECOS.2013.22-3.12

García, G., & Muñoz-Vera, A. (2015). Characterization and evolution of the sediments of a Mediterranean coastal lagoon located next to a former mining area. *Marine Pollution Bulletin*, *100*(1), 249–263. https://doi.org/10.1016/J.MARPOLBUL.2015.08.042

Köppen, G. W. (1936). *Handbuch der Klimatologie in fünf Bänden Das geographische System der Klimate*. www.borntraeger-cramer.com

Lakshmi, A., & Rajagopalan, R. (2000). Socio-economic implications of coastal zone degradation and their mitigation: a case study from coastal villages in India. *Ocean & Coastal Management*, *43*(8–9), 749–762. https://doi.org/10.1016/S0964-5691(00)00057-0

Le Moigne, F. A. C., Henson, S. A., Sanders, R. J., & Madsen, E. (2013). Global database of surface ocean particulate organic carbon export fluxes diagnosed from the ^{234}Th technique. *Earth System Science Data*, *5*(2), 295–304. https://doi.org/10.5194/essd-5-295-2013

Maderich, V., Kim, K. O., Brovchenko, I., Jung, K. T., Kivva, S., & Kovalets, K. (2022). Dispersion of Particle-Reactive Elements Caused by the Phase Transitions in Scavenging. *Journal of Geophysical Research: Oceans*, *127*(10). https://doi.org/10.1029/2022JC019108

Marco, F., Marín, M. D., & Castillo, L. G. (2016). Estudio del transporte de sedimentos en la Rambla del Albujón. *Anuario de Jóvenes Investigadores*, *9*, 74–77.

Marín-Guirao, L., Atucha, A. M., Barba, J. L., López, E. M., & García Fernández, A. J. (2005). Effects of mining wastes on a seagrass ecosystem: metal accumulation and bioavailability, seagrass dynamics and associated community structure. *Marine Environmental Research*, *60*(3), 317–337. https://doi.org/10.1016/J.MARENVRES.2004.11.002

Martínez Fernández, J., & Esteve Selma, M. A. (2003). *El papel de las aguas subterráneas en la exportación de nutrientes de origen agrícola hacia la laguna del Mar Menor*.

Mirion. (2024). *Lab Experiment 7: High-Resolution Gamma-Ray Spectroscopy with HPGe Detectors*. https://www.mirion.com/discover/knowledge-hub/articles/education/high-resolution-gamma-ray-spectroscopy-with-hpge-detectors-lab-experiments

MITECO. (1999). *Zonas Especialmente Protegidas de Importancia para el Mediterráneo*. https://www.miteco.gob.es/en/biodiversidad/temas/espacios-protegidos/espacios-protegidos-por-instrumentos-internacionales/en_ap_zepim.html

Moore, R. M., & Hunter, K. A. (1985). Thorium adsorption in the ocean: reversibility and dis~ibution amongst particle sizes. *Geochimica et Cosmochimica Acta*, *49*, 2253–2257.

Muir, G. K. P., Pates, J. M., Karageorgis, A. P., & Kaberi, H. (2005). ^{234}Th:^{238}U disequilibrium as an indicator of sediment resuspension in Thermaikos Gulf, northwestern Aegean Sea. *Continental Shelf Research*, *25*(19–20), 2476–2490. https://doi.org/10.1016/j.csr.2005.08.009

Newton, A., Brito, A. C., Icely, J. D., Derolez, V., Clara, I., Angus, S., Schernewski, G., Inácio, M., Lillebø, A. I., Sousa, A. I., Béjaoui, B., Solidoro, C., Tosic, M., Cañedo-Argüelles, M., Yamamuro, M., Reizopoulou, S., Tseng, H.-C., Canu, D., Roselli, L., … Khokhlov, V. (2018). Assessing, quantifying and valuing the ecosystem services of coastal lagoons. *Journal for Nature Conservation*, *44*, 50–65. https://doi.org/10.1016/j.jnc.2018.02.009

NOAA. (2023, March 28). *Sea Water | National Oceanic and Atmospheric Administration*. https://www.noaa.gov/jetstream/ocean/sea-water

NOAA. (2024). *Planoply 4.1.1*.

Not, C., Brown, K., Ghaleb, B., & Hillaire-Marcel, C. (2012). Conservative behavior of uranium vs. salinity in Arctic Sea ice and brine. *Marine Chemistry*, *130–131*, 33–39. https://doi.org/10.1016/J.MARCHEM.2011.12.005

Owens, S. A., Buesseler, K. O., & Sims, K. W. W. (2011). Re-evaluating the ^{238}U-salinity relationship in seawater: Implications for the ^{238}U– ^{234}Th disequilibrium method. *Marine Chemistry*, *127*(1–4), 31–39. https://doi.org/10.1016/J.MARCHEM.2011.07.005

Owens, S. A., Pike, S., & Buesseler, K. O. (2015). Thorium-234 as a tracer of particle dynamics and upper ocean export in the Atlantic Ocean. *Deep-Sea Research Part II: Topical Studies in Oceanography*, *116*, 42–59. https://doi.org/10.1016/j.dsr2.2014.11.010

Oyarzun, R., Manteca Martínez, J. I., López García, J. A., & Carmona, C. (2013). An account of the events that led to full bay infilling with sulfide tailings at Portman (Spain), and the search for "black swans" in a potential land reclamation scenario. *Science of the Total Environment*, *454–455*, 245–249. https://doi.org/10.1016/j.scitotenv.2013.03.030

Pates, J. M., & Muir, G. K. P. (2007). U–salinity relationships in the Mediterranean: Implications for ^{234}Th:^{238}U particle flux studies. *Marine Chemistry*, *106*(3–4), 530–545. https://doi.org/10.1016/j.marchem.2007.05.006

Perez-Ruzafa, A. (1989). *Estudio ecológico y bionómico de los poblamientos bentónicos del Mar Menor (Murcia, SE de España)*.

Perez-Ruzafa, A., & Aragón, R. (2002). Implicaciones de la gestión y el uso de las aguas subterráneas en el funcionamiento de la red trófica de una laguna costera. *Conflictos Entre El Desarrollo de Las Aguas Subterráneas y La Conservación de Los Humedales: Litoral Mediterráneo*, 215–245.

Pérez-Ruzafa, Á., Marcos, C., & Gilabert, J. (2005). The ecology of the Mar Menor coastal lagoon: a fast changing ecosystem under human pressure. In *Coastal lagoons. Ecosystem processes and modeling for sustainable use and development* (pp. 392–422).

Pérez-Ruzafa, A., Navarro, S., Barba, A., Marcos, C., Cámara, M. A., Salas, F., & Gutiérrez, J. M. (2000). Presence of Pesticides throughout Trophic Compartments of the Food Web in the Mar Menor Lagoon (SE Spain). *Marine Pollution Bulletin*, *40*(2), 140–151. https://doi.org/10.1016/S0025-326X(99)00193-9

Rodellas, V., Roca-Martí, M., Puigcorbé, V., Castrillejo, M., & Casacuberta, N. (2023). Radionuclides as ocean tracers. In *Marine Analytical Chemistry* (pp. 199–273). Springer International Publishing. https://doi.org/10.1007/978-3-031-14486-8_4

Romero Díaz, A., Pedraza Caballero, A., & Pérez Morales, A. (2017). Expansión urbana y turismo en la Comarca del Campo de Cartagena-Mar Menor (Murcia). Impacto en el sellado del suelo. *Cuadernos de Turismo*, *39*(39), 521–546. https://doi.org/10.6018/TURISMO.39.290691

RStudio Team. (2020). *RStudio: Integrated Development Environment for R*. http://www.rstudio.com/

Ruiz, J. M., Albentosa, M., Aldeguer, B., Álvarez-Rogel, J., Antón, J., Belando, M. D., Bernardeau, J., Campillo, J. A., Domínguez, J. F., Ferrera, I., Fraile-Nuez, E., García, R., Gómez-Ballesteros, M., Gómez, F., González-Barberá, G., Gómez-Jakobsen, F., León, V. M., López-Pascual, C., Marín-Guirao, L., … Yebra, L. (2020). *Informe de evolución y estado actual del Mar Menor en relación al proceso de eutofización y sus causas. Informe de asesoramiento técnico del Instituto Español de Oceanografía (IEO).*

Santos-Echeandía, J., Bernárdez, P., & Sánchez-Marín, P. (2023). Trace metal level variation under strong wind conditions and sediment resuspension in the waters of a coastal lagoon highly impacted by mining activities. *Science of the Total Environment*, *905*. https://doi.org/10.1016/j.scitotenv.2023.167806

Santschi, P. H., Li, Y.-H., & Bell, J. (1979). Natural radionuclides in the water of Narragansett Bay. *Earth and Planetary Science Letters*, *45*(1), 201–213. http://inis.iaea.org/search/search.aspx?orig_q=RN:11535327

Tudela, A., & Delgado, A. (2019, October). *Mar Menor: historia profunda de un desastre*.

Turner, R. K., Subak, S., & Adger, W. N. (1996). Pressures, trends, and impacts in coastal zones: Interactions between socioeconomic and natural systems. *Environmental Management*, *20*(2), 159–173. https://doi.org/10.1007/BF01204001/METRICS

UPCT. (2024). *Mar Menor Data*. https://marmenor.upct.es/charts/

Velasco, J., Lloret, J., Millan, A., Marin, A., Barahona, J., Abellan, P., & Sanchez-Fernandez, D. (2006). Nutrient and particulate inputs into the Mar Menor lagoon (Se Spain) from an intensive agricultural watershed. *Water, Air, and Soil Pollution*, *176*(1–4), 37–56. https://doi.org/10.1007/s11270-006-2859-8

Waples, J. T., Benitez-Nelson, C., Savoye, N., Rutgers van der Loeff, M., Baskaran, M., & Gustafsson, Ö. (2006). An introduction to the application and future use of ^{234}Th in aquatic systems. *Marine Chemistry*, *100*(3–4), 166–189. https://doi.org/10.1016/J.MARCHEM.2005.10.011

8 APPENDIX

8.1. ADDITIONAL INFORMATION

Table 1. Coordinates of the stations and time of CTD's deployment in the four stations.

Station	Coordinates	Time of CTD's deployment
M1	37°47'15.07"N, 0°46'59.34"W	2024/25/01 09:23:12
M2	37°43'25.50"N, 0°47'16.44"W	2024/25/01 10:40:24
M3	37°40'27.28"N, 0°46'23.27"W	2024/25/01 11:44:44
M4	37°41'40.60"N, 0°49'9.77"W	2024/25/01 12:43:11

Table 2. Percentage of the ^{234}Th activity in the particulate fraction regarding the total (dissolved + particulate). Mean and standard deviation calculated from all depths sampled in each station.

	M1	M2	M3	M4	Mean
0 m	9%	10%	31%	40%	22%
1 m	14%	17%	34%	57%	30%
2 m	-	20%	-	74%	47%
3 m	21%	30%	36%	61%	37%
4 m	0%	23%	11%	48%	20%
5 m	-	25%	9%	-	17%
Mean	11%	21%	24%	56%	28%
Standard deviation	9%	7%	13%	13%	20%

8.2. SALINITY YSI DATA CORRECTION

Figure 14 showing salinity profiles in each M1, M2, M3 and M4 sampling locations. Orange line representing original salinometer (YSI) data registered during the field trip vs. darker line representing CTD salinity data. To try to correct the YSI data, the average and standard derivation of the difference between YSI and CTD from all collected data were calculated and then applied to the original YSI values (blue line).

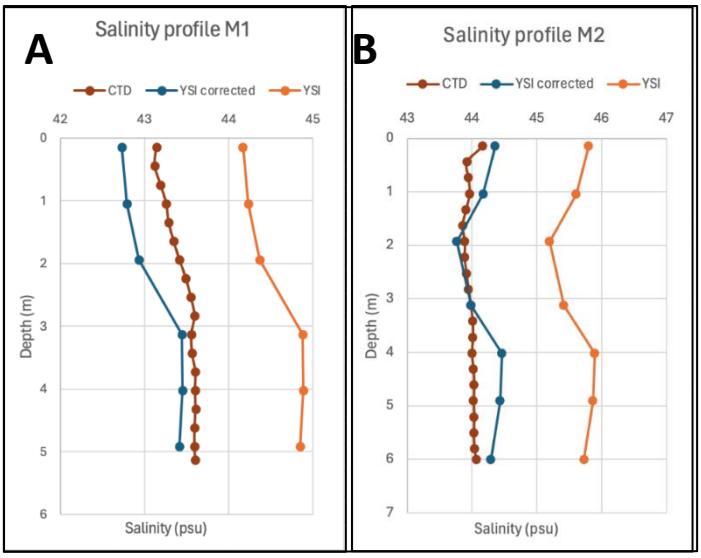

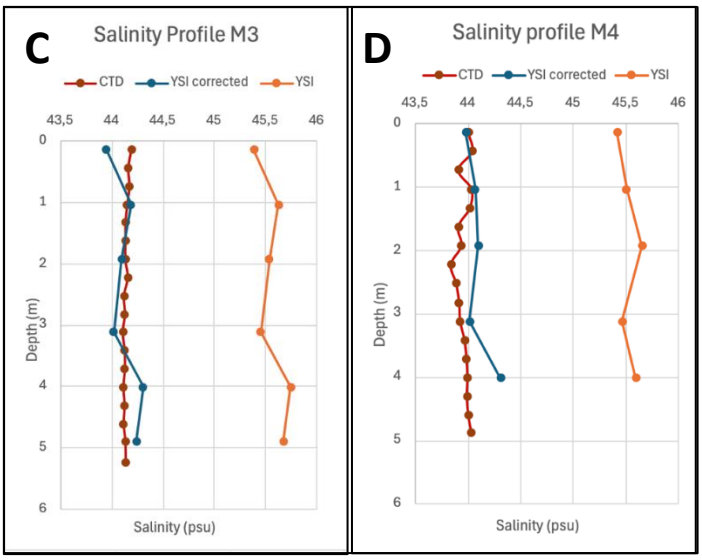

Figure 14. Salinity profiles in each station, M1, M2, M3 and M4 corresponding to panels A, B, C and D respectively. Red line shows CTD's salinity, blue shows salinometer's salinity corrected with the standard deviation and orange line shows salinometer's original salinity

8.3. TOTAL SAMPLE PROCESSING CLEVENGER ET AL. (2021)

Appendix B: ^{234}Th 2L Ship Procedure Quick Guide

1. Sampling:
    a. Label 2L bottles (grey tape/sharpie)
    b. Rinse 2L bottles 3x with seawater and dump rinses
    c. Fill 2L bottles with SW sample to overflow, then **remove 20 mL** with pipette
2. Add **~3.5 mL of conc. HNO_3** to bring pH to ~1.5 in 2L bottles, do not shake
3. Add **1 mL of ^{230}Th** with auto-pipette, don't use first 3/last 3 mL, shake 10x
4. Let sit for **6 hours**
5. Add **~3.5 mL of NH_4OH** to bring **pH to 8-8.5**, shake 10x, use pH meter, record pH
6. Add **100 µL of $KMnO_4$** solution, shake 10x
7. Add **100 µL of $MnCl_2$** solution, shake 10x
8. Let sit for **8 hours** (to form manganese ppt)
9. Place 25 mm QMA in filter head, screw onto 2L bottle, label filter head
10. Invert 2L bottle slowly, place in rack, attach octopus at same time as opening the valve, immediately crack open the filter head (at the bottle-head connection) to release pressure
11. Record start and stop times of filtering, at the end close the valve and remove from rack
12. Lightly place filter head in bench-top rig (don't jam down, will puff up QMA)
13. Open valve while rinsing salts away 3x with **pH 9 water** (fill 1 L bottle with MQ, 1 drop NH_4OH)
14. Remove QMA, place in labeled petri dishes, let dry for several hours at 60 °C
15. Mount QMA in the following order: mount, QMA, 1 mylar, 2 aluminum foil, mount ring
16. Trim mount, label, beta count
17. Rinse 2L bottles and filter heads with **rinse solution** (928 mL MQ + 63 mL conc HNO_3 + 10 mL 30% H_2O_2 OR 990 mL 1N HNO_3, 10 mL 30% H_2O_2), then rinse 3x with freshwater

8.4. TURBIDITY AND CHLOROPHYLL FIGURES

January 23rd turbidity (Figure 15) and chlorophyll concentration (Figure 16) figures:

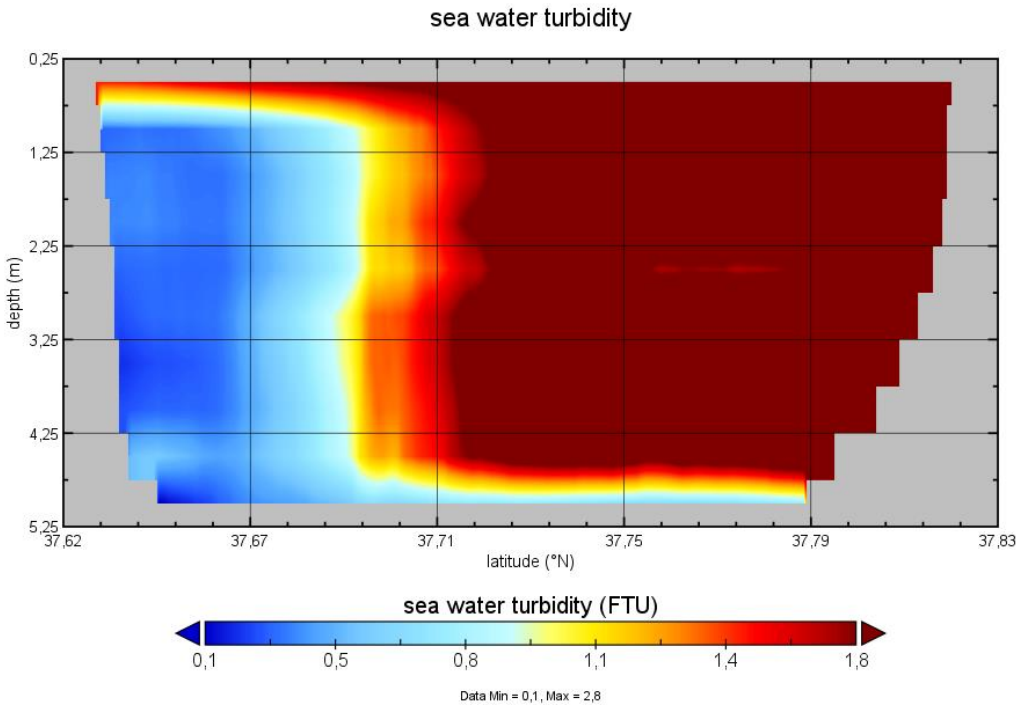

Figure 15. Seawater turbidity on January 23rd. Data from (UPCT, 2024), and processed with Planoply 4.1.1 (NOAA, 2024)

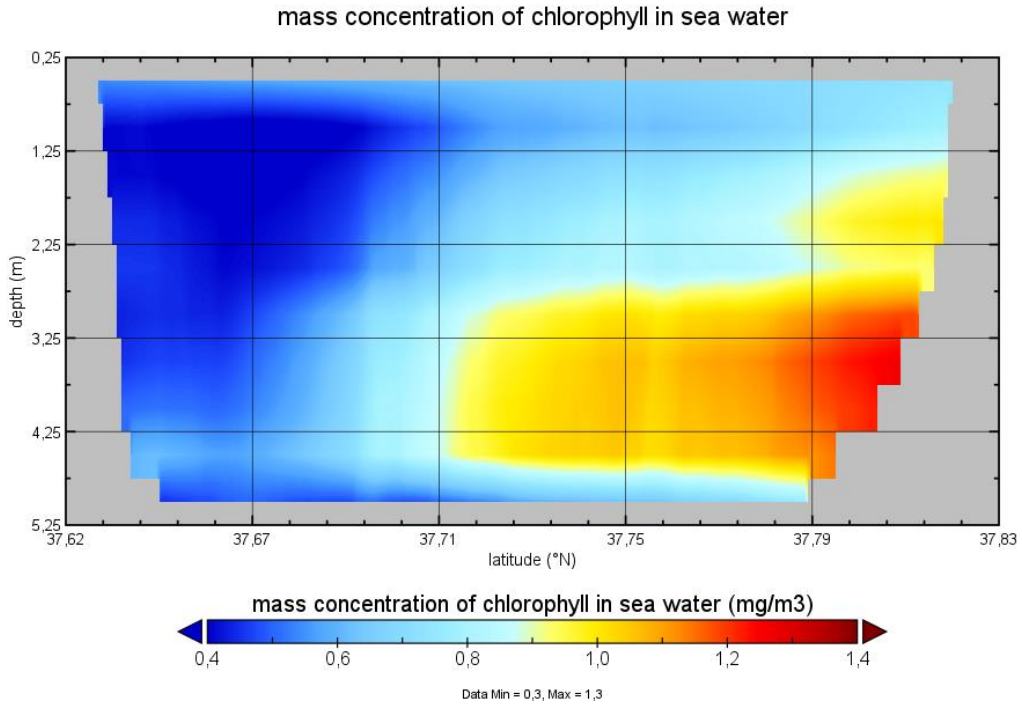

Figure 16. Concentration of chlorophyll in seawater on January 23rd. Data from (UPCT, 2024), and processed with Planoply 4.1.1 (NOAA, 2024)

February 1st turbidity at 4.0 m figure:

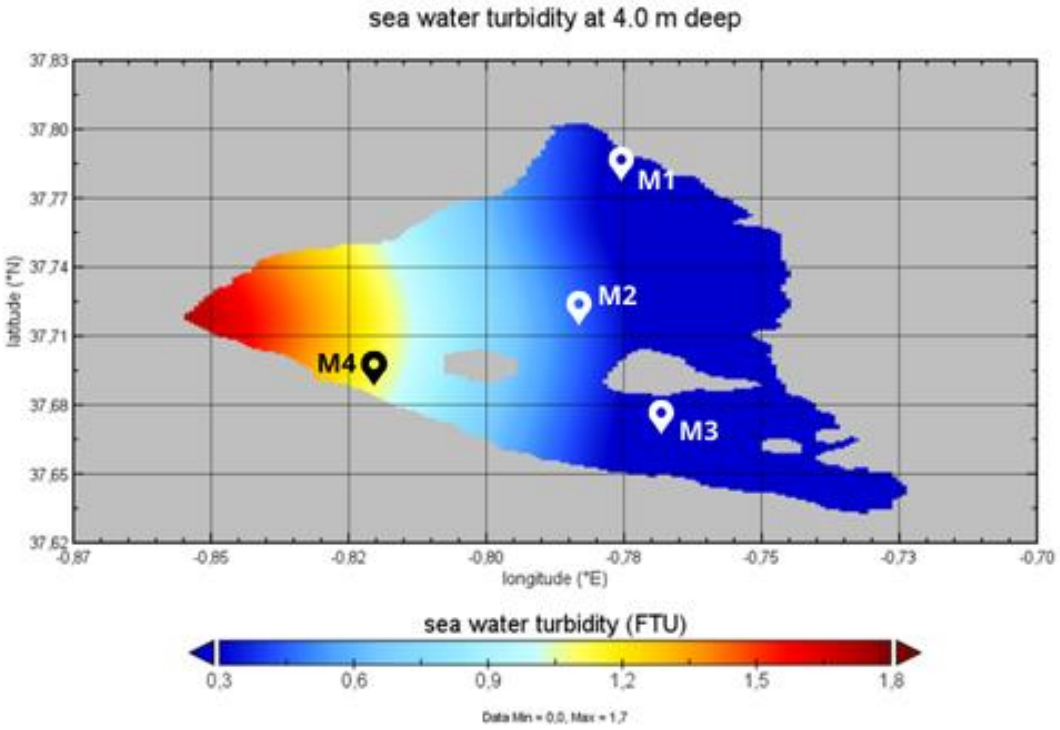

Figure 17. Seawater turbidity at 4.0 m deep along Mar Menor on February 1st, stations marked as dots. Data from (UPCT, 2024), and processed with Planoply 4.1.1 (NOAA, 2024)

.

8.5. ^{234}Th Flux calculation

Table 3. Data showing ^{234}Th flux calculation for all stations following Rodellas et al. (2023). ^{234}Th deficit is calculated by subtracting ^{234}Th measured activity to ^{238}U measured activity. Layer thickness is calculated by using a midpoint integration method. Integrated ^{234}Th deficit is obtained in each layer by multiplying ^{234}Th deficit and layer thickness. Finally, flux for each station is obtained by multiplying the sum of integrated ^{234}Th deficit by the decay constant of ^{234}Th (λ_{Th} = 0.02876 day^{-1}). A: M1, B:M2, C:M3 and D:M4.

A

Station	Depth	Th-234 measured activity (dpm L-1)	U-238 measured activity (dpm L-1)	Th-234 deficit (dpm L-1)	Layer thickness (m)	Integrated Th-234 deficit (dpm m L-1)
M1	0	0.46	3.08	2.62	0.5	1.31
M1	1	0.37	3.09	2.72	1.5	4.08
M1	2					
M1	3	0.43	3.11	2.68	1.5	4.02
M1	4	0.72	3.11	2.39	1.8	4.30
M1	5					
	5.3					
					5.3	**13.71**
					Flux at 5.3m (dpm m-2 day-1)	**394**

B

Station	Depth	Th-234 measured activity (dpm L-1)	U-238 measured activity (dpm L-1)	Th-234 deficit (dpm L-1)	Layer thickness (m)	Integrated Th-234 deficit (dpm m L-1)
M2	0	0.40	3.16	2.75	0.5	1.38
M2	1	0.35	3.14	2.79	1	2.79
M2	2	0.51	3.14	2.62	1	2.62
M2	3	0.34	3.14	2.81	1	2.81
M2	4	0.49	3.14	2.65	1	2.65
M2	5	0.53	3.15	2.62	1.8	4.71
M2	6					
	6.3					
					6.3	**16.96**
					Flux at 6.3m (dpm m-2 day-1)	**488**

C

Station	Depth	Th-234 measured activity (dpm L-1)	U-238 measured activity (dpm L-1)	Th-234 deficit (dpm L-1)	Layer thickness (m)	Integrated Th-234 deficit (dpm m L-1)
M3	0	0.36	3.16	2.80	0.5	1.40
M3	1	0.56	3.16	2.60	1.5	3.90
M3	2					
M3	3	0.58	3.15	2.57	1.5	3.85
M3	4	0.64	3.15	2.51	1	2.51
M3	5	0.57	3.15	2.58	1.3	3.36
	5.8					
					5.8	**15.02**
					Flux at 5.8m (dpm m-2 day-1)	**432**

D

Station	Depth	Th-234 measured activity (dpm L-1)	U-238 measured activity (dpm L-1)	Th-234 deficit (dpm L-1)	Layer thickness (m)	Integrated Th-234 deficit (dpm m L-1)
M4	0	0.50	3.14	2.65	0.5	1.32
M4	1	0.51	3.15	2.64	1	2.64
M4	2	0.31	3.14	2.83	1	2.83
M4	3	0.36	3.14	2.77	1	2.77
M4	4	0.44	3.14	2.71	1.4	3.79
	4.9					
					4.9	**13.36**
					Flux at 4.9m (dpm m-2 day-1)	**384**

8.6. WORK PLAN

SCHEDULE PROGRAM	month	SEPT.		OCTOBER				NOVEMBER				DECEMBER				JANUARY				FEBRUARY				MARCH				APRIL				MAY				JUNE				JUL.
	week	3	4	1	2	3	4	1	2	3	4	1	2	3	4	1	2	3	4	1	2	3	4	1	2	3	4	1	2	3	4	1	2	3	4	1	2	3	4	1
1. FIRST STEPS																																								
Topic assingment and introduction																																								
Bibliographic research																																								
Schedule and target establishment																																								
Elaborating an outline plan																																								
Planning campaign and preparation																																								
2. PROJECT DEVELOPMENT																																								
Objectives																																								
Introduction																																								
Mar Menor campaign execution																																								
Methods																																								
Post-campaign sample processing																																								
First project submission																																								
Sample results analysis and first hypothesis																																								
Results																																								
3. PROJECT COMPLETION																																								
Discussion and conclusions																																								
Second project submission																																								
First project defense																																								
Future perspectives																																								
Final project submission																																								
Final defense and end of the project																																								

8.7. Relació del TFG amb els estudis de Grau de CCAA de la UAB

La gran majoria dels ecosistemes presents al nostre planeta, per aparentment remota que sigui la seva localització, ja no es troben completament aïllats. La presència d'activitats antròpiques s'estén arreu dels cinc continents, especialment en el que es refereix a l'ús dels recursos que la natura ofereix: ja siguin béns explotables, sòl sobre el que construir o desenvolupar activitats agrícoles i ramaderes o oceans que proveeixen de recursos i aliment a la població mundial.

La convivència d'espais naturals i desenvolupament d'activitats socio-econòmiques ha acabat per deteriorar ecosistemes complexos i d'especial interès com ho són ara les llacunes costaneres. Aquest estudi, centrat en el Mar Menor, un dels espais naturals protegits més importants de la Península Ibèrica i la llacuna costanera més gran d'Europa, pretén reflectir la greu problemàtica que sofreix aquesta llacuna i sobretot, que és possible una remediació d'aquest espai si es desenvolupen i s'aposta per l'ús de tècniques innovadores per al seu estudi.

Les creixents i continues pressions antròpiques que ha sofert aquest paratge al llarg dels segles ha resultat en el col·lapse de l'ecosistema agreujant cada cop més els efectes sobre la biodiversitat que l'habita. La necessitat de regulació i protecció d'espais només serà efectiva quan co-existeixi amb un estudi eficaç de causes i conseqüències dels processos que hi prenen lloc. En aquest cas concret, el desenvolupament d'una eina poc coneguda en aquest camp podria obrir un nou camí per comprendre millor les dinàmiques que determinen els fluxos de partícules de la llacuna, podent arribar a aplicar-les en estudis per a relacionar aquests fluxos amb grans episodis catastròfics com els viscuts els darrers anys. L'ús de radionúclids i en especial del parell $^{234}Th/^{238}U$ podria esdevenir un punt clau, no només en aquest cas concret sinó en altres amb condicions similars, per a poder traçar partícules d'origen natural i contaminants entenent millor els ecosistemes i podent aplicar per tant mesures eficaces per a la seva conservació.

Aquest estudi interdisciplinari relaciona la necessitat de nocions bàsiques sobre física de radionúclids, oceanografia, legislació i coneixement d'espais naturals protegits, tècniques de laboratori per al processament de mostres i altres conceptes relacionats amb la química de l'aigua. Totes adquirides a través de les diferents assignatures del grau de Ciències Ambientals, el qual, a més d'oferir coneixements d'unes bases científiques, defensa la importància de conscienciació del medi natural que ens envolta atenent a la necessitat d'harmonia entre les activitats antròpiques desenvolupades i les limitacions i la capacitat de resiliència del medi que ens rodeja.